journal of the international meteor organization

WGN

43:1
february 2015

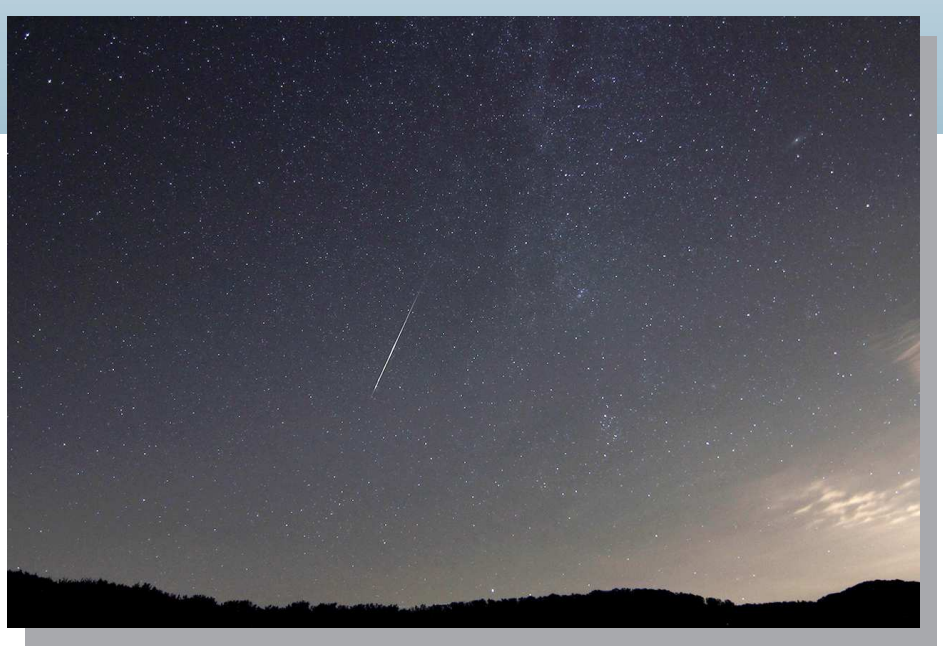

IMC 2015 announcement
IMO's new online fireball form
Recurrent showers and some minor showers
September–October video meteors

ISSN 1016-3115

WGN Vol. 43, No. 1, February 2015, pp. 1 – 40

Administrative

Conferences

Meteor Science

Preliminary results

Front cover photo

Meteor captured during an early Perseid watch form the Jura mountains (Switzerland) on 2013 August 3 at $22^{h}30^{m}$ UT using Canon EOS 7D with 14 mm $f/2.8$ lens and 30 s exposure at ISO 1600. Photo courtesy: Jonas Schenker.

Back cover photo

Meteoroids approach the Earth from different directions. Individual radiants are points on the sky from which they are approaching. Particles belonging to a meteoroid stream have similar orbits and therefore form radiants near to each other. This area is a radiant of a meteor shower. Meteoroids come to the Earth from a so-called geocentric radiant. Directions of meteors observed from Earth's surface are given as result of vector sum of meteoroid's and Earth's motion. The dominant motion is that of the Earth around the Sun, a smaller part is also due to Earth's rotation and gravitation. Thus meteors come from directions called apparent radiants. Distribution of sporadic radiants is given as apparent. On this figure positions are plotted of the apparent radiants of meteor showers relative to Sun. Positions of radiants are plotted in steps of one day during all period of activity. Positions at maxima are presented by larger circles. Author: Peter Zimnikoval.

Writing for WGN

This Journal welcomes papers submitted for publication. All papers are reviewed for scientific content, and edited for English and style. Instructions for authors can be found in WGN **31:4**, 124–128, and at `http://www.imo.net/docs/writingforwgn.pdf` .

Copyright

Legal address

International Meteor Organization, Jozef Mattheessensstraat 60, 2540 Hove, Belgium.

Janus

Cis Verbeeck[1]

Another year has passed. 2014 was a year full of interesting papers and presentations about meteor science. Especially the rich return of video meteor observations and their catalogs was ubiquitous. The IMC in Giron was a great meeting where meteor workers from around the globe presented their interesting work, shared experiences, and made bold new plans for the future. At this occasion, Jürgen Rendtel's long career as IMO President was celebrated with a nice reception.

After a lot of work from several authors and from editors Jürgen Rendtel and Rainer Arlt, a new edition of the Handbook for Meteor Observers was introduced at the IMC in Giron. In fact, the handbook is now split into two parts: the Handbook for Meteor Observers and the Meteor Shower Workbook 2014 (which is expected to be updated more frequently than the Handbook for Meteor Observers). A lot of copies have been sold since.

2014 also saw the revival respectively the demise of some of IMO's Commissions. Bill Ward became the new Director of the Photographic Commission. While this Commission was in dormant mode for many years as video observations gained terrain on photographic observations, there is an important place for still image meteor photography with a DSLR. Bill has described in WGN how you can contribute to the various goals of the Photographic Commission. Furthermore, Bill organized an informal meeting about the Photographic Commission after hours at the IMC, which drew 22 interested participants and addressed topics like image formats, image verification, copyright issues, metadata, and automatic linking to fireball sightings. We expect the Commission to boom when the new IMO website will be in place, allowing easy uploads of photographs and metadata.

Since no single telescopic meteor observation was reported to IMO in the past ten years, the Commission Director Malcolm Currie acknowledged that this way of observing meteors has become obsolete. Together with him, the Council decided to abolish the Telescopic Commission. IMO's FIreball DAta Center FIDAC has also been virtually out of business for the past years and was abolished as well. Behind the scenes however, Mike Hankey and Vincent Perlerin have been working hard to set up an online multi-language fireball form that has been translated into over 25 languages with the help of many IMO members. The form is very intuitive and has the potential to reach a large public of "ordinary" people in each of those language groups. It is released right now as you can read elsewhere in the present issue of WGN!

I gladly take the opportunity to announce that Megan Argo will henceforth be IMO's Press Officer. She will write and distribute press releases when opportunities arise, like a big fireball or meteorite fall, or a major shower maximum like the Perseids or Geminids. She will regularly write news items for the IMO website and post meteor content on IMO's Facebook and Twitter accounts. One of her first assignments will be the press release in English about IMO's online fireball form, to be sent out in conjunction with the next big fireball or so that will attract the attention of journalists. We will count on the enthusiasm of local groups to translate this press release into their own language so they can send it to their local press.

In 2015, the IMO Council will issue a survey about IMO, which is intended to gauge what IMO members and other meteor enthusiasts feel about IMO, what they expect from IMO, what are IMO's current strengths and weaknesses, and what can be improved.

One of the most exciting projects that start in 2015 is building a brand new IMO website. Mike Hankey, Vincent Perlerin, and Roman Piffl will start working on the new website soon, in collaboration with the IMO Council. The discussions during the dedicated workshop at the IMC in Giron provided a good starting point for this task.

2015 will also see the next round of Council elections, for the term 2016–2019. If you want to contribute actively to IMO and care about its activities and future health, you are invited to consider being a candidate for the Council. IMO needs a healthy mix of old and new Council members that share and discuss their visions of where IMO should be heading, with a passion to help implement their ideas. More information will follow in the April issue of WGN.

I wish all readers a happy, healthy, and successful 2015, full of clear skies, fireballs and meteor fun!

Janus *was a Roman god with two faces, one looking to the past and one to the future, called upon at the beginning of any enterprise. Today he is often a symbol of re-appraisal at the start of the year.*

[1] Bogaertsheide 5, 2560 Kessel, Belgium.
Email: cis.verbeeck@scarlet.be

IMO bibcode WGN-431-verbeeck-janus NASA-ADS bibcode 2015JIMO...43....1V

IMO's new online fireball form

Mike Hankey[1] *and Vincent Perlerin*[2]

Introduction

The American Meteor Society (AMS) has accepted reports of suspected fireballs and bolides from the general public from as far back as 1922 (Olivier, 1922) and online since 2005. The online fireball report form has been specifically designed to be usable by people with no astronomy experience who witnessed a fireball, a bolide or a suspected similar phenomenon. This online form is a part of the *Citizen Science* movement where novices and amateurs contribute to the scientific research of our field. This form is also an educational tool as it helps the users understand what they saw.

At the request of the IMO Council, the online Fireball report form has been adapted to an IMO version for a wider audience and translated in 28 of languages so far (Arabic, Bulgarian, Czech, Danish, German, English, Spanish, French, Hebrew, Croatian, Japanese, Lithuanian, Norwegian, Dutch, Polish, Brazilian Portuguese, Portuguese, Romanian, Russian, Slovakian, Slovenian, Cyrillic Serbian, Serbian, Swedish, Turkish, Ukrainian, Simplified Chinese and Traditional Chinese).

The new form is accessible at `http://fireballs.imo.net`.

Collected data and interaction

The form is divided into 12 easy-to-fill steps. When possible, the steps present graphical interactive elements that help the users give the most precise and exhaustive information about their sighting. The graphical interactive elements allow the user to give useful information without having to fully understand scientific concepts such as *azimuth* or *stellar magnitude*. For each step, the user is assisted by videos and/or help text.

The IMO Fireball Report Form allows collecting the following information:

- **Location of the witness at the time of the event**
  (latitude, longitude, altitude, state or region and country)
  The location information is processed through the Google Map API. After entering an address, the user moves an icon on an interactive map to the exact location where he witnessed the phenomenon (Figure 1). The latitude, longitude, altitude and administrative information (region, state, etc.) are automatically gathered from a Google service.

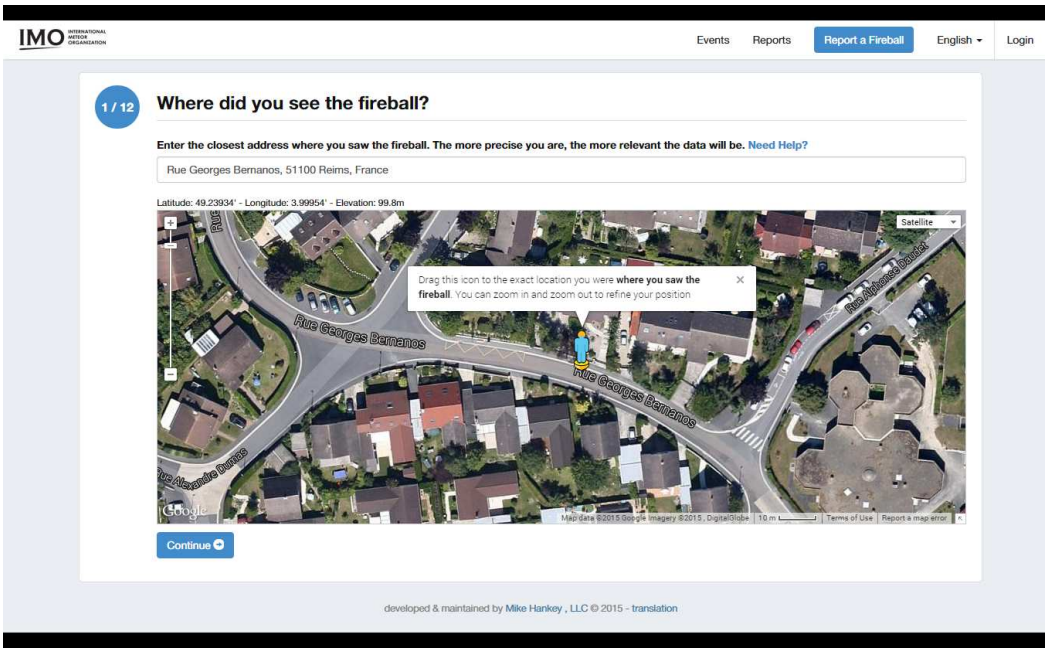

Figure 1 – Step 1: Location of the witness.

- **Date, time and duration of the sighting**
  (local date and time, duration and UT date and time)
  The UT date and time are automatically obtained from the Google Time Zone API service from the latitude, the longitude and the local date and time shared by the user (Figure 2).

[1]Email: `mike.hankey@gmail.com`
[2]Email: `vperlerin@gmail.com`

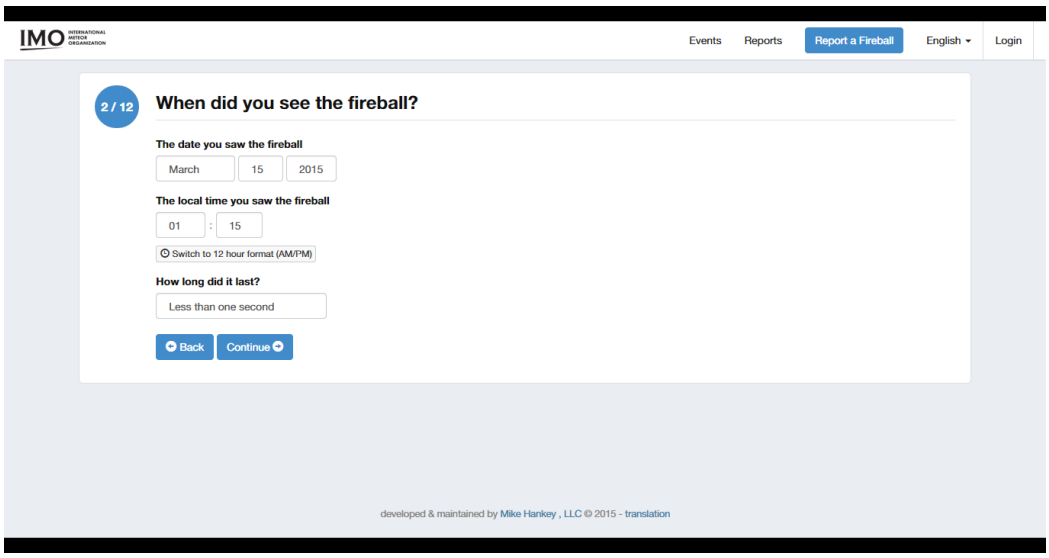

Figure 2 – Step 2: Date, time and duration.

- **Descent angle**
  During the IMC 2013 in Poznan, Peter Jenniskens suggested the AMS form could be improved by asking the witness the approximate descent angle of the bolide instead of the general direction (from top left to bottom right, from top right to bottom left, etc.) This has been implemented in the IMO version of the form: using a simple slider, the user rotates a representation of a fireball to the angle he saw (Figure 3).

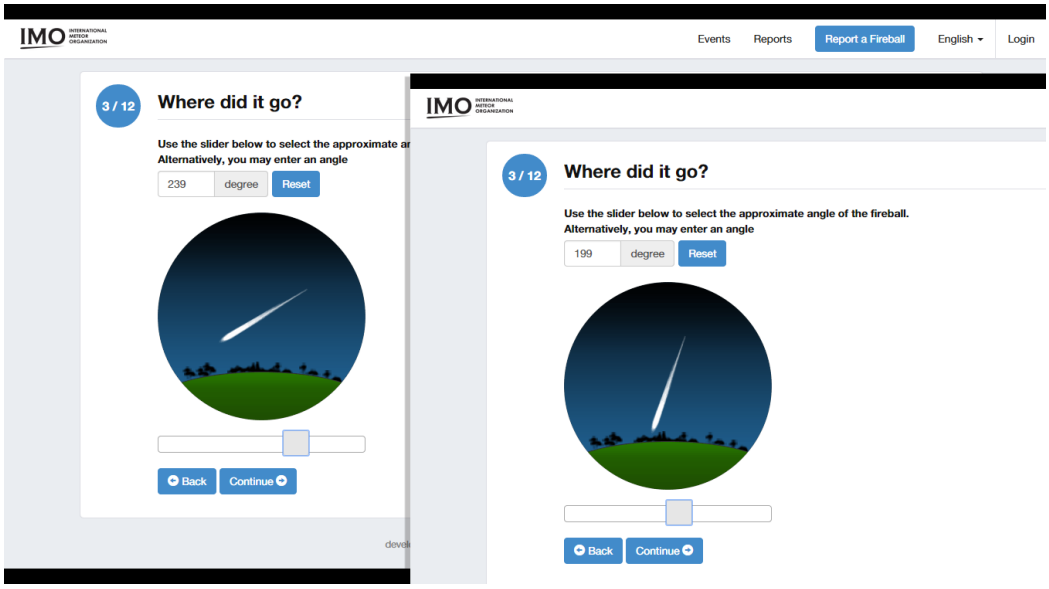

Figure 3 – Step 3: Descent angle.

- **Facing azimuth**
  The user gives his facing azimuth during the sighting by moving an arrow on the same map used on Step 1 (Figure 4).
- **Starting and ending elevation and azimuth**
  The user shares the initial and final azimuth and elevation of the phenomenon he saw using the same interactions (mouse click on a map and sliding, see Figures 5 and 6).
- **Stellar magnitude and color(s)**
  Stellar magnitude is very hard to evaluate for a non-trained user. To help the user to share this information, we use a graphical scale from "As Bright as Venus" to "As Bright as the Sun" (Figure 7).
- The form also allows the user to give information as text:
  - **Train information (duration, length)**
  - **Terminal flash and fragmentation (occurrence, description)**

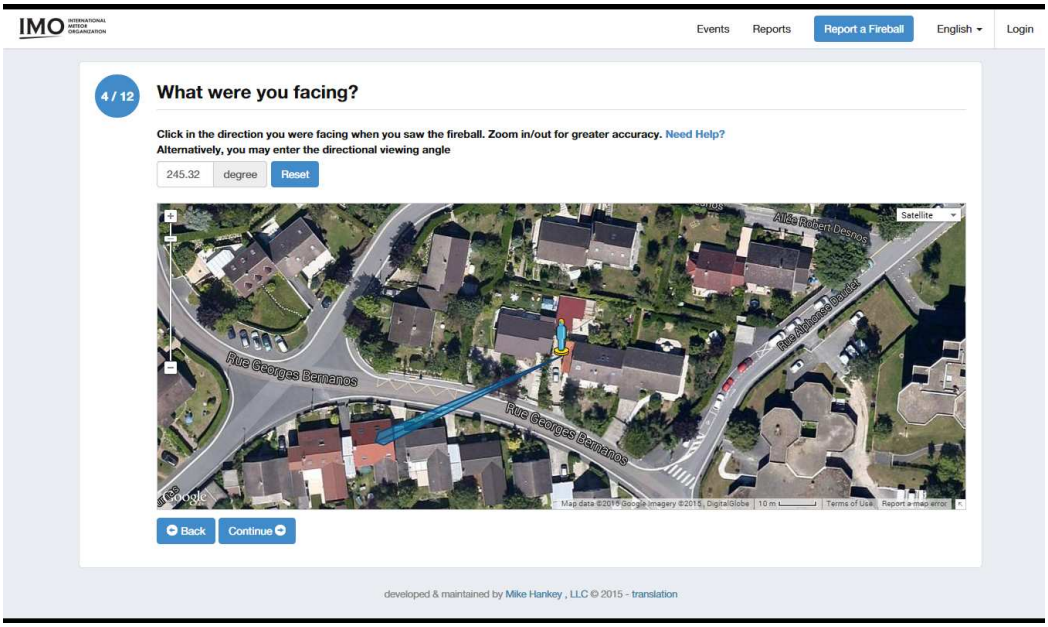

Figure 4 – Step 4: Facing azimuth.

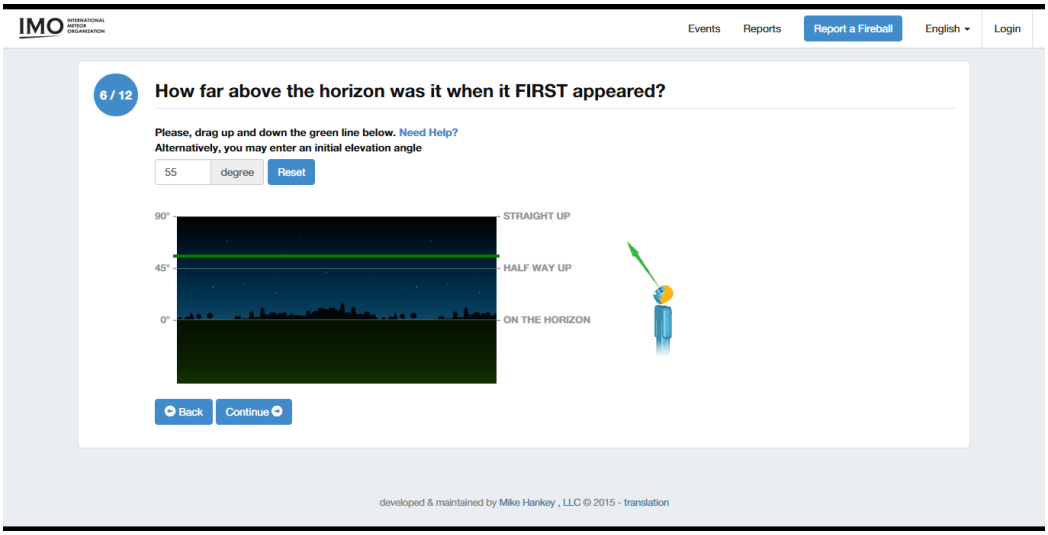

Figure 5 – Step 6 (and 8): Elevations.

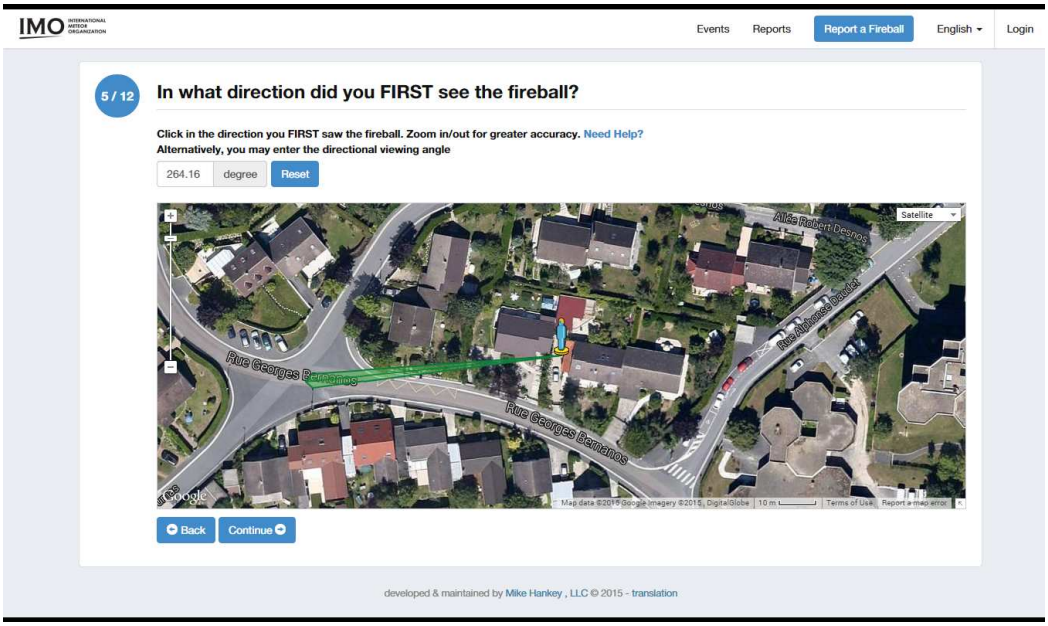

Figure 6 – Step 5 (and 7): Azimuths.

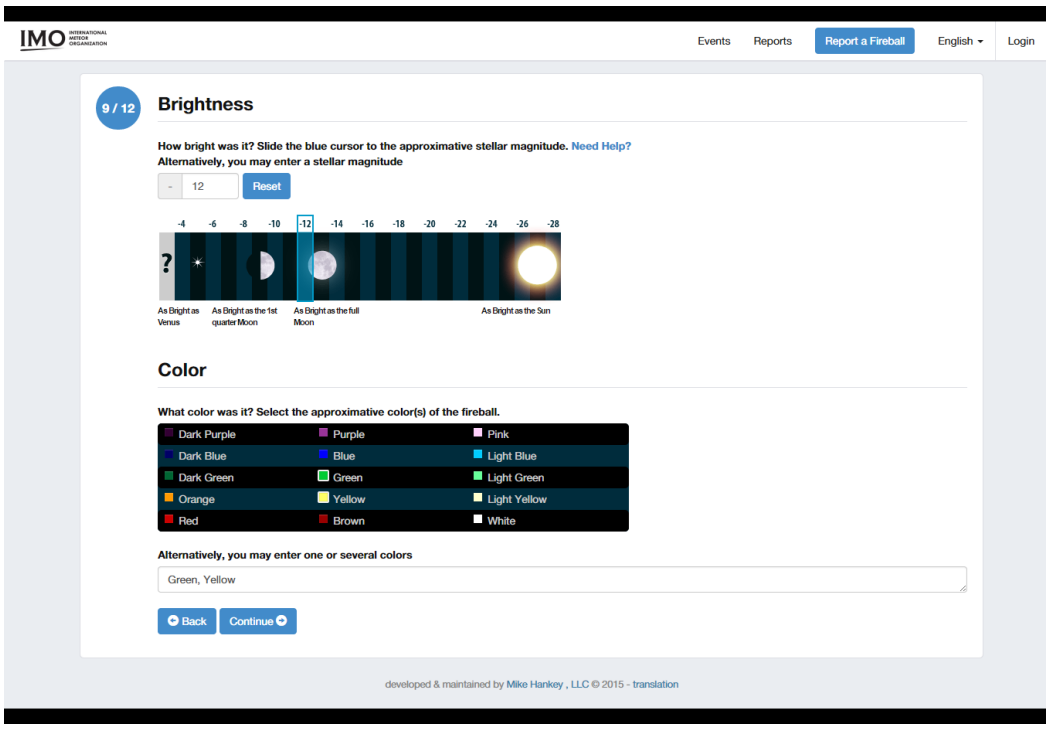

Figure 7 – Step 9 : Brightness and colors.

– **Sonic effect (concurrent and/or delayed sound – time, duration and description)**

– **Contact information of the witness**
The contact information of the witness allows the IMO to ask for precision about each sighting when needed. User first name and last name remain hidden from the public area of the site.

Events map and admin area

All the reports are analyzed in the admin area of the site. The reports are grouped into events based on the location of the witnesses and the time of the sighting. The IMO team averages all the times collected to obtain a common time for each event. This common time can be validated against satellite re-entries and recorded fireball events and found to be accurate usually within a few minutes of the reality.

The IMO team has access to the admin area of the site where the reports can be grouped into events or invalidated. The list of pending reports (Figure 8) is sorted by UT date and time of the sightings. The system automatically detects reports that can be linked to an existing event. The detection is based on the comparison of the UT date and time of the report and the average UT date and time of the event.

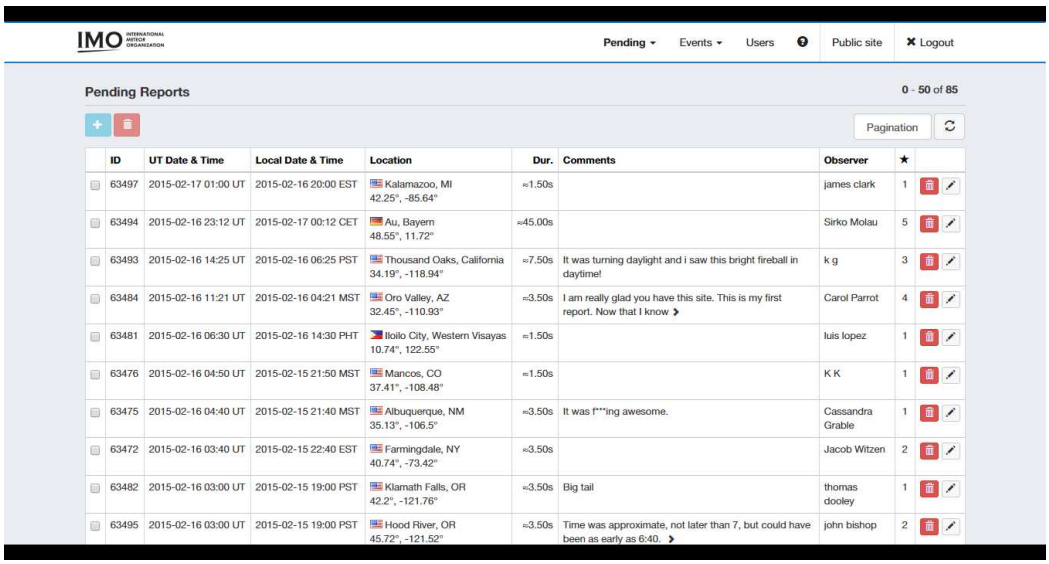

Figure 8 – Admin area: Pending reports.

Figure 9 – Admin area: Pending report with potentially related event.

In order to help the administrator, the following information is displayed in this case (Figure 9):

- The time difference (in hours and minutes) between the report and the potentially related event
- The distance (in km) from the average position of all the witnesses of the event (called "Epicenter" on the interface) and the position of the witness of the current report.

The administrator can also search for all the pending reports that are potentially linked to an existing event. This function should be very useful if a huge number of reports are posted at the same time after a particularly big event.

The events are published on the site along with a map displaying the witness location, sighting vectors and all the details provided by the witnesses (Figure 10).

Reports with sonic effect are often indicative of meteorite dropping fireballs. Knowing the time difference between the sighting and the sound gives clues about where the meteoroid exploded and where meteorites could possibly be found on the ground.

Evaluation

Since 2005, the AMS has received over 46 600 reports and 34 788 individual events. About 75% of the reports have been approved and grouped into events. A detailed quantitative evaluation of the form can be found on the AMS website. As it is impossible to predict the success of the IMO version of the form, the success of the AMS

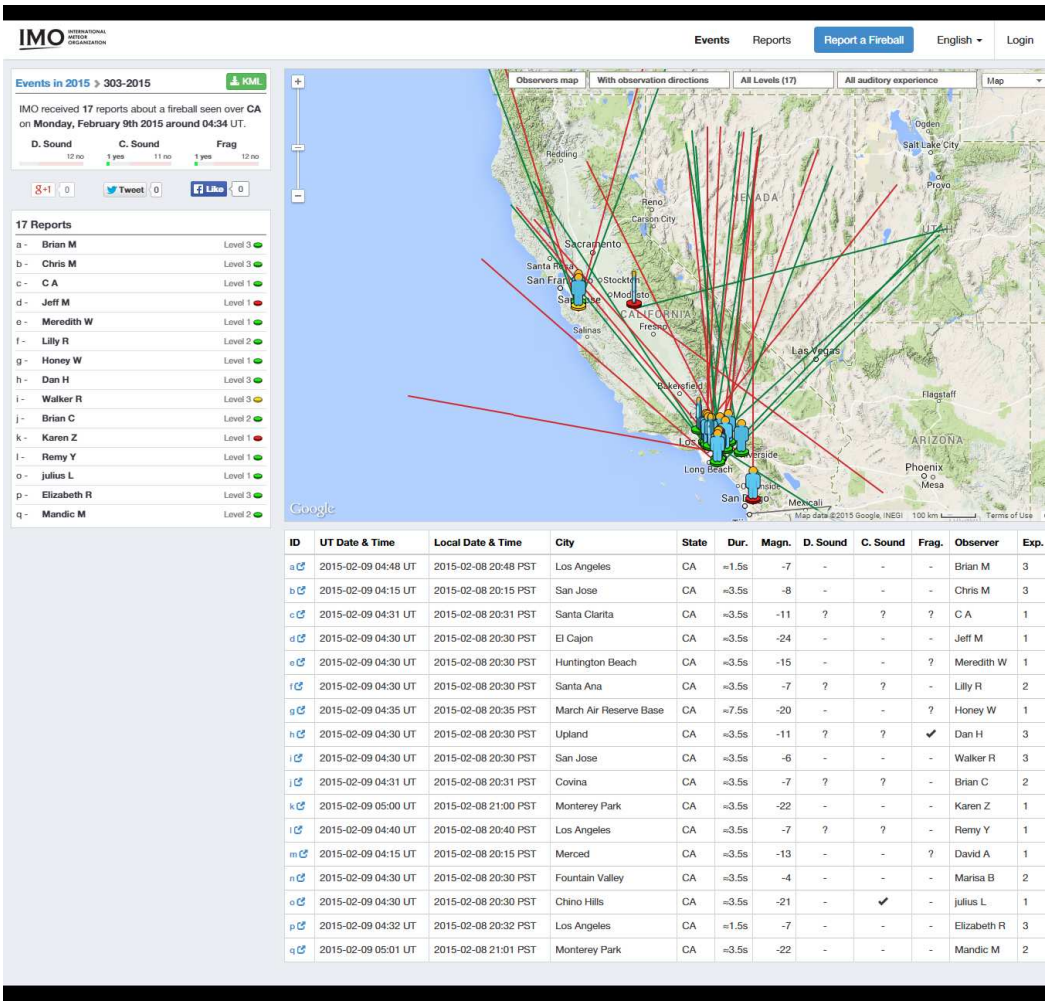

Figure 10 – Event map.

version shows at least the form is perfectly usable by novices. Between 2012 October 13 and 2015 February 17, 950 visitors evaluated the form. 93.72% of these visitors found the form "Good" or "Outstanding."

The scientific community and various government agencies including NASA, the Coast Guard, and the Air Force have successfully used the AMS Fireball log for different purposes. We are convinced the international version (the IMO version) could have the same success towards various international and national organizations.

Several meteorite recoveries have occurred in part due to the data collected by the AMS and the AMS fireball reports have assisted meteor and meteorite research at NASA Ames and other NASA offices (Hankey et al., 2013). The re-entry of satellites and space debris has been confirmed by AMS reports. The Coast Guard has also used the AMS reports to vet calls about crashed airplanes off the coast of Florida (which later turned out to be fireball meteors). The data collected by the IMO and the AMS fireball forms will be saved in a common database for further analysis.

Note

As this form is new and covers a broad range of languages there is the potential for grammatical errors or other bugs. We encourage all IMO members to test the new form and proof read the text in their native language. If you want to update a translation or create a new one, please, follow the instructions on `http://fireballs.imo.net/members/imo/translators` web page, or contact the authors directly.

List of languages and translators

Below is the list of the people who helped translating the IMO fireball form:

- Abderrahmane Ibhi (Arabic)
- Valentin Velkov (Bulgarian)
- Ladislav Bálint (Czech)
- Anton Sørensen (Danish)
- Andre Knöfel (German)
- Mike Hankey & Vincent Perlerin (English – original version)
- Francisco Ocaña González (Spanish)
- Vincent Perlerin and Karl Antier (French)
- Arie Blumenzweig (Hebrew)
- Denis Vida and the Višnjan School of Astronomy (Croatian)
- Masahiro Koseki (Japanse)
- Audrius Dubietis (Lithuanian)
- Trond Erik Hillestad (Norwegian)
- Paul Roggemans (Dutch)
- Przemysław Żołądek (Polish)
- Eduardo Placido Santiago (Brazilian Portuguese)
- Carlos Saraiva (Portuguese)
- Adriana Roggemans (Romanian)
- Marian Stasjuk (Russian)
- Roman Piffl (Slovakian)
- Javor Kac (Slovenian)
- Snežana Todorović (Serbian and Cyrillic Serbian)
- Johan Kero (Swedish)
- Ferhat Fikri Özeren (Turkish)
- Pavel Presnyakov (Ukrainian)
- Wu BingXun (Simplified and Traditional Chinese)

References

Hankey M., Perlerin V., Lunsford R., and Meisel D. (2013). "American Meteor Society online fireball report". In Gyssens M., Roggemans P., and Żołądek P., editors, *Proceedings of the International Meteor Conference, Poznań, Poland, 22–25 August 2013*. IMO, pages 115–119.

Olivier C. P. (1922). "The great meteor of May 11, 1922". *Popular Astronomy*, **33**, 502–503.

IMO bibcode WGN-431-hankey-fireballs NASA-ADS bibcode 2015JIMO...43....2H

Conferences

International Meteor Conference 2015, 34th edition, August 27–30, Mistelbach, Austria

Thomas Weiland[1]

Period and location

The International Meteor Conference 2015, organized by the *Wiener Arbeitsgemeinschaft für Astronomie (Vienna Astronomy Association – WAA)* will be held at Mistelbach, Austria from August 27 (Thursday evening) until August 30 (Sunday lunchtime).

Mistelbach is a small town (11 000 inhabitants), some 45 km north-north-east of the capital of Austria, Vienna, and 25–30 km from the Czech and Slovakian border (see Figure 2). It is situated in the "Weinviertel" district of Lower Austria, a hilly area characterized by crop fields and vineyards, small patches of forest and lanes with old cellar houses ("Kellergassen") at the outskirts of quiet villages (see IMC 2015 logo – Figure 1).

Mistelbach offers dry continental conditions, more related to the Eastern Czech Republic, Western Slovakia and Hungary than to the wet Atlantic climate in Western Austria, especially the Alpine Regions. Winters are sometimes cold and summertime can be pretty hot (maximum temperatures often exceeding +30 °C, even at the end of August).

Figure 1 – The IMC 2015 logo.

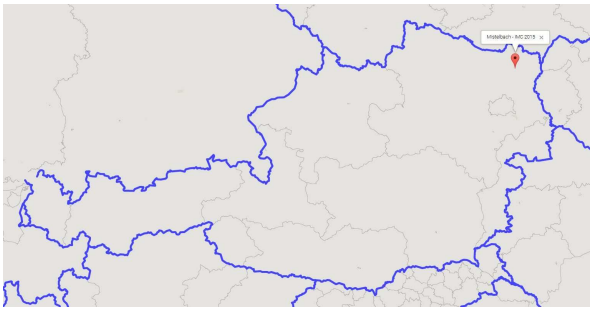

Figure 2 – Location of Mistelbach within the boundaries of Austria.

Conference venue and accommodation

Contrary to the first announcement, the conference will now be held at the *MAMUZ Museum Mistelbach*, only a few minutes walk from the *Landwirtschaftliche Fachschule (Agricultural School)*, which still serves as host for full-board-participants. Both sites are not far from the town's centre.

The *MAMUZ Museum Mistelbach* comprises two sites suitable for lectures and the poster session. The "Kapelle – Chapel" (see Figure 3, left and middle) has all facilities essential for a modern day lecture room (beamer, projection screen, curtains for darkening, cooling etc.), with a capacity of 120 people. The nearby "M-Zone" (see Figure 3, right) will serve as restaurant and host the poster session during the conference.

With its capacity of 96 beds (32 triple rooms) the school (see Figure 4) has enough space for housing most of the participants. The remaining will be accommodated on private basis in Mistelbach and nearby villages. There is even a public camp ground in Poysdorf, about 10 minutes by car from Mistelbach. All rooms at the school offer basic facilities with shower / WC (see Figure 5). Breakfast (buffet) will be served at the school's dining room for full-board-participants (see Figure 6).

Figure 3 – MAMUZ Museum Mistelbach, "Chapel" (left), "Chapel", lecture room (middle) and the "M-Zone" (right).

[1]Ospelgasse 12-14/6/19, 1200 Wien, Austria. Email: thomas.weiland@aon.at

Programme and social events

Lectures
Lectures will have a duration of 10 to 30 minutes. Each lecture must allow 2–3 minutes for questions or comments.

Posters
Posters are welcomed and offer an opportunity to present special topics not suitable for a lecture and for participants not willing to give an oral presentation respectively.

Proceedings
All contributions to the conference, both lectures and posters, should find their way to the IMC Proceedings, either as a paper or at least as an abstract. Therefore the contributors are strongly advised to have the paper ready before their talk or poster presentation. Articles should be written according to the instructions published on the IMC 2015 website. A template in Word is available. All papers of the IMC Proceedings will be registered in the Harvard-NASA Astrophysic Data System.

Workshops
Since a lot of like-minded people will come together during the conference it seems fairly easy to organize extra sessions dedicated to special topics. Workshops can take place outside the official IMC programme, in the evening hours, but it is possible to hold them before or after the IMC.

SOC
In order to guarantee the high quality of the presentations all of them have to be registered before the IMC and will be supervised by a team of IMO members. This Scientific Organizing Committee (SOC) will compile the conference programme and the content of the IMC Proceedings.

Socializing
It can't be stressed enough – socializing is one of the main goals of an IMC. Therefore the conference programme will reserve enough time for personal contacts during the opening reception, the Saturday afternoon excursion, breaks and evenings at the bar, including music sessions.

Figure 4 – Agricultural School, entrance.

Figure 5 – Agricultural School, part of triple room.

Figure 6 – Agricultural School, part of dining room.

Excursion to NHM / Saturday evening programme

On Saturday afternoon an excursion is planned to the *Naturhistorisches Museum Wien (NHM)* (`http://www.nhm-wien.ac.at`).

The *Museum of Natural History in Vienna* hosts the largest and probably most important meteorite collection in the world (it contains about 8500 objects, most of them historical falls, of which about 1100 are shown to the public). A guided tour with a meteorite expert will be offered. Special attention is paid to a recently donated lunar rock sample and the purchased Martian meteorite *Tissint*, whose fall was observed by nomads in Morocco in 2011. It is the fifth documented fall of a Martian meteorite and the second largest one from Mars ever found. With a mass of nearly 1 kilogram the museum owns the biggest single piece of that find.

The visit to the NHM will start with two buses (the total number of attendants is limited to 120) just after lunch at 1 pm, arrival at the museum is scheduled at 2 pm. To avoid crowding the number of participants is split. During the last hour everyone has the opportunity to explore the collections of the museum on their own.

At 5 pm we will return to Mistelbach and visit a *"Heuriger"*, a typical wine restaurant, which is, with respect to its socializing effect, comparable to the English Pub to some extent. The *"Heuriger"* lies very close to the *Agricultural School*. There a special closing dinner (cold buffet) will be served.

Thursday / Friday non-astronomical programme

To give the participants an impression of the countryside surrounding Mistelbach a non-astronomical programme (rides in a horse-drawn carriage, guided tours through "Kellergassen"; see chapter "Period and location") will be offered during the opening reception on Thursday afternoon.

The other part of the non-astronomical programme will take place on Friday afternoon and includes a visit of the historical royal castle *Schönbrunn* and the adjacent (historical) zoo. The latter is especially suitable for families with children.

Further details of the Thursday / Friday non-astronomical programme will be announced in a future issue of WGN, via newsletters and on the IMC 2015 website: `http://www.imo.net/imc2015/`.

Travel information

Mistelbach is well connected to other parts of Lower Austria and the capital Vienna by train and bus. There are also bus connections to the nearby Czech Republic and Slovakia as well as to Hungary.

Travelling by plane

From Vienna International Airport

The most convenient way to come by plane to Mistelbach is via *Vienna International Airport (VIE)*. The airport is connected to all major parts of the world. From there you have to take a train (*Schnellbahn Line S 7*) to the station *Wien Praterstern*, which is a 30 minutes trip (train service roughly every half an hour). From *Wien Praterstern* you have to catch another train to Mistelbach (*Schnellbahn Line S 2*). There are plenty of such trains to Mistelbach and the trip takes about 1 hour. In addition you can choose between the *Schnellbahn Line S 2* and local trains, especially during rush hours. The LOC will organize a free shuttle service from Mistelbach railway station to the *Agricultural School* and to private accommodations respectively. Let the LOC know when you will arrive in Mistelbach.

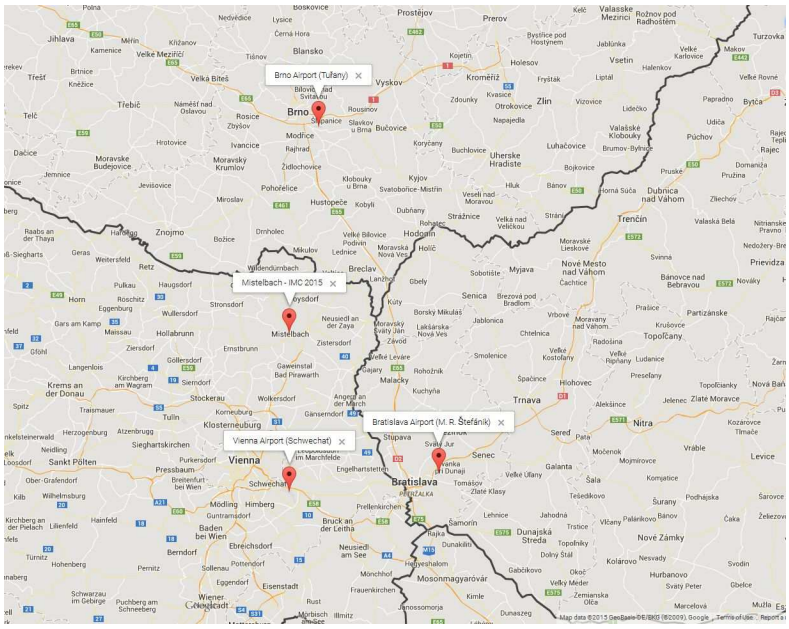

Figure 7 – Airports near Mistelbach.

A word of warning: alternatively to the *Schnellbahn Line S 7* there is another train service to the city of Vienna, called *City Airport Train (CAT)*. This train is faster (16 minutes duration), but rather expensive (€11.- instead of €4.40; one way). It has its terminal at *Wien Mitte*, from where not as many trains are going to Mistelbach as from *Wien Praterstern*. Therefore it is recommended to take the *Schnellbahn Line S 7* and change the train at *Wien Praterstern*.

From Bratislava International Airport

Bratislava International Airport (BTS) is the second largest international airport in the vicinity of Mistelbach and may be a cheaper option, especially for Eastern European residents. The airport is connected with *Bratislava hlavná stanica* (Bratislava main railway station) via Bus Line 61 (service every 15–20 minutes). From there a train going to *Wien Hauptbahnhof* (Vienna main railway station) leaves roughly every hour and the trip takes 1 hour and 15 minutes. *Wien Hauptbahnhof* is connected with *Wien Praterstern* by *Schnellbahn Lines S 1, S 2 and S 3* (service every 5–10 minutes; 12 minutes duration).

From Brno International Airport

Brno International Airport (BRQ) is the third international airport not far away from Mistelbach. Although the airport is frequented by some cheap airlines, it is not recommended to fly via Brno, since there is no direct train connection to Mistelbach. There is a bus service from Brno to Vienna, which stops at Mistelbach, but only one time a day. The latter applies for the way back, too.

Travelling by train
If you intend to go by train to Mistelbach you have to integrate Vienna in your itinerary. Vienna's main railway station (*Wien Hauptbahnhof*) is connected with all major European cities. After arriving at *Wien Hauptbahnhof* you have to follow the route described in chapter "Travelling by plane".

Travelling by bus
Vienna is also connected with many European cities by bus. *Eurolines Austria* for instance starts and ends at the *Vienna International Busterminal (VIB)*, from where you have to go by *Underground Line U 3 (orange) and U 1 (red)* to *Wien Praterstern* and catch a train to Mistelbach then (see chapter "Travelling by plane").

Travelling by car
Mistelbach lies very close to motorway A 5 (*Nord Autobahn*) between Vienna and Schrick, where it changes into B 7 (*Brünner Straße*) to Mistelbach.

1. If you come from the west (Salzburg, Linz):
   You take motorway A 1 (*West Autobahn*) until the junction St. Pölten, where you change to S 33 (*Kremser Schnellstraße*). At the junction Jettsdorf you turn into S 5 (*Stockerauer Schnellstraße*) and go as far as the junction Stockerau. From there follow A 22 (*Donauufer Autobahn*) until the junction Korneuburg and change to S 1 (*Wiener Außenring Schnellstraße*). At the junction Eibesbrunn you turn into A 5.

2. If you come from the north (Czech Republic):
   In that case it is recommended to enter Austria at the international checkpoint Mikulov / Drasenhofen. From there you go on B 7 (*Brünner Straße*) to Mistelbach.

3. If you come from the east (Slovakia, Hungary):
   Coming from Slovakia you enter Austria at the international checkpoint Jarovce / Kittsee. From there you take motorway A 6 (*Nordost Autobahn*) until the junction Bruckneudorf, where you change to motorway A 4 (*Ost Autobahn*). You follow the motorway until the junction Prater (in Vienna) and change to motorway A 23 (*Autobahn Südosttangente Wien*) in direction to Brno / Praha. The A 23 merges with S 2 (*Wiener Nordrand Schnellstraße*) and further on becomes S 1 (*Wiener Außenring Schnellstraße*). At the junction Eibesbrunn you turn over to A 5.
   Coming from Hungary you enter Austria at the international checkpoint Hegyeshalom / Nickelsdorf. From there you take motorway A 4 (*Ost Autobahn*) until the junction Prater, where you turn into motorway A 23.

4. If you come from the south (Klagenfurt, Graz):
   You take motorway A 1 (*Südautobahn*) until the junction Inzersdorf-West (in Vienna). You keep the direction and change to motorway A 23 (in direction to Kaisermühlen).

Carpooling
Sharing a car with others can help to reduce the number of cars and travelling costs and stimulate socializing as well. Therefore carpooling is encouraged by the LOC. For privacy reasons information about the travel plans of participants will be displayed in a limited way. So, if you want to share a car with others let the LOC know, and it will bring you in contact with the right person.

Registration

Registration fee
Until 2015 May 31 the standard registration fee is €150.- and €180.- after this date. The registration deadline is 2015 July 15. Non-accommodated participants are charged €100.- until May 31 and €130.- after this date. Private accommodations can be booked by the LOC, but have to be paid together with the non-accommodation fee in advance (see registration form).

Because of limited space at the MAMUZ Museum Mistelbach please note that the number of participants is restricted to 120!

According to that, registration policy will be "first come, first served".

The standard registration fee includes 3 nights of accommodation in a triple room (Thursday, August 27 to Sunday, August 30) at the *Agricultural School*, full board (breakfast, lunch and dinner; except beverages other than plain water), all IMC lectures and the poster session, coffee breaks, the excursion to the NHMW and the Saturday evening programme ("Heuriger"), T-shirt, conference material and the IMC proceedings. Unless the "no accommodation" option is chosen, accompanying persons older than 12 years sharing a room with a participant also have to register as such. Contact the LOC if you need an alternative accommodation and do not forget to tell with whom you want to share a room.

The non-accommodation fee comprises all conference benefits except accommodation and breakfast. Prices for private accommodations including breakfast mostly range from ca. €21.- to €53.- for double rooms and from ca. €24.- to €66.- for single rooms (all prices are per night, per person).

Extra nights
Participants who want to come earlier or stay longer can reserve extra nights (see registration form). You can choose between triple, double or single rooms (including breakfast) at the *Agricultural School* and private accommodations (with or without breakfast) in Mistelbach and surrounding villages respectively. Lunch and dinner has to be chosen on site. Extra rooms can only be booked together with the IMC registration until July 15. After this date participants should book on their own behalf any extra nights. Triple, double and single rooms at the *Agricultural School* are only available from August 25 to August 26 and from August 31 to September 04 and, concerning triple and double rooms, if participants register together.

Cancellation policy

- until 2015 May 31: full reimbursement, reduced by a cancellation fee of €15.-
- from June 1 until July 15: partial reimbursement of €75.-
- from July 15: no reimbursement.

Information and contact details

For further information, updates, latest details, registration and payment please check the IMC 2015 website: `http://www.imo.net/imc2015/`. Any other inquiries should be made via Email: `imo2015@imo.net`. You can also contact the Local Organizing Committee (LOC) by telephone:

Thomas Weiland
+43 0676-8118-96402

Anneliese Haika
+43 0676-4122849

Thomas Maca
+43 0699-19444930

Nick Heyworth
+43 0699-81181250

Christoph Niederhametner
+43 0680-3044195

Hope to see you in Mistelbach!

IMO bibcode WGN-431-weiland-imcann NASA-ADS bibcode 2015JIMO...43....8W

International Meteor Conference
2015 August 27–30, Mistelbach, Austria
Registration form

Do not use if you have internet access! Please register electronically on `http://www.imo.net/imc2015` if you can. Only if you have **no** internet access, fill out one form for each individual participant and return it to Marc Gyssens, IMO Treasurer, Heerbaan 74, B-2530 Boechout, Belgium, as soon as possible. Registration will be guaranteed only after the IMO Treasurer has received the full registration fee for the option chosen. We expect this payment has been made when this form was sent. All IMC payments are due at registration without any delay.

Name: _____ Address: _____

_____

Phone: _____ Fax: _____ E-mail: _____

Date of birth:† _____

- I wish to register for the IMC 2015 from August 27 to 30:
  - ○ I opt for the standard fee (150 EUR early/180 EUR late);
  - ○ I opt for the non-accommodation fee (100 EUR early/130 EUR late) plus private accommodation (has to be payed together with the registration fee – please contact the LOC for details;)
  - ○ I opt for arranging my own accommodation (100 EUR early/130 EUR late).
- I prefer to share a room with _____ (if applicable).
- T-shirt: Size (S–M–L–XL–XXL): _____ Gender: _____ (included in fee)
- Food requirements (e.g., vegetarian, nut allergy): _____
- I intend to travel by _____, together with _____
- I will arrive at _____ (e.g. Aug.27 15h), and my departure is _____ (e.g. Aug.30 14h).
- I need extra nights for the dates ___ (e.g. Aug.25–26) in a single or double or triple room (mark choice).

For participants wishing to contribute to the programme (please include your lecture or poster abstract):

Lecture (title and author(s)): _____

Duration: _____ minutes (including a few minutes for questions and discussion)

Poster(s): _____ Space: _____ m^2

Paper delivery date: No paper Before IMC During IMC Before 15 September Before 30 September

Comments:

- ○ I am paying the entire registration fee for the option selected.
- ○ I acknowledge having read and I agree with the cancellation policy.
- ○ † Under aged participants must be accompanied by parents or have a legal authorization document. Inform yourself with your local authorities about the law applicable for under-aged persons travelling abroad. Formalities may require legalized documents provided by local authorities or a notaire and may require time to be prepared. Ignoring procedures defined in law, your journey to an IMC risks to be stopped at the airport or at the border.

The indicated amount should be sent to the IMO via one of the payment options. The following payment options are available:

- **International bank transfer** to the International Meteor Organization, Mattheessensstraat 60, B-2540, Hove, Belgium, IBAN account number: BE30 0014 7327 5911, BIC bank code: GEBABEBB (Fortis Bank, Belgium). This is recommended for people living in the European Union, as it is no more costly than a domestic bank transfer when done correctly.
- **PayPal payment** to `payment@imo.net`. In that case, we must ask you to add the costs involved in the transaction (3.4% of the total sum including costs, plus 0.35 EUR).
- **Other arrangements**. Please contact the IMO Treasurer for information.

Meteor Science

Various meteor scenes III: Recurrent showers and some minor showers

Masahiro Koseki[1]

Meteor activities vary widely from year to year. We study here the June Bootids (JBO), τ-Herculids (TAH), and Andromedids (AND) which are basic examples for the recurrent nature of meteor showers. Half a century has passed since well-known photographic or radar meteor showers were detected. It is necessary to note that some 'established' IAU showers are historical ones and we cannot always see them. We find the historical trace of AND by video and four distinct activities in the area of JBC (=JBO+TAH).
Meteor showers look different by different observational techniques. Many minor showers in the IAU list have been detected only by observations stored for many days and many years; visual observations in a single night cannot perceive them naturally. We studied the ϕ-Piscids (PPS), χ-Taurids (CTA), γ-Ursae Minorids (GUM), η-Pegasids (ETP), and α-Sextantids (ASX) as examples and found they have not been recognized by visual observers at all. It is noteworthy that some of them have possible identifications in the IAU list and in preceding observations or reports. The difference in search methods makes the situations much more complicated. The five minor showers we studied here do not have confirmations by all observational techniques.
Geobased search (radiant point, time of the observation, and possibly geocentric velocity) may overlook showers which are dispersed in radiant position. A search using the D-criterion is dependent on the presumption of a spherical distribution in the orbital space and may not represent the real distribution, or may overestimate the accuracy of the observations and lead to subdividing the showers into several parts. We must use these search methods properly.

Received 2014 February 28

1 Winneckids and 73P/Schwassmann-Wachmann 3 related activity

Different parent bodies are thought to produce different meteor showers. A meteor shower was predicted from 7P/Pons-Winnecke and some observers detected the outburst, moreover, followed by recurrent displays (Hashimoto & Osada, 1998). A meteor shower was predicted from comet 73P/Schwassmann-Wachmann 3 and many faint meteors were recorded by a sensitive observer (Nakamura, 1930; Jenniskens, 2006, p. 392). Those two events are distinguishable naturally in the historical record but how we see them now is quite different. We call them with neighbor activities the June Bootid Complex (= JBC).

The author discovered a remarkable meteor activity (Koseki, 1982; 1986; 2009; Table 1) around the two historical showers but it does not have a clear center. Figure 1 shows the distribution of the photographic meteor radiants within $55 \leq \lambda_{\odot} < 100°$; circle size represents the similarity, i.e. circle radius is inversely proportional to $D(M, N)$ from the mean orbit of MK-49 and small circles are not members of MK-49. The members of this shower are spread all over this figure and, moreover, one of them is beyond the frame. Visual observers could not recognize its activity or detect the radiant. We could not detect any activity by the definition on the radiant distribution and, therefore, we must use the geobased or the orbbased method (see Koseki, 2014a = Paper I) appropriately.

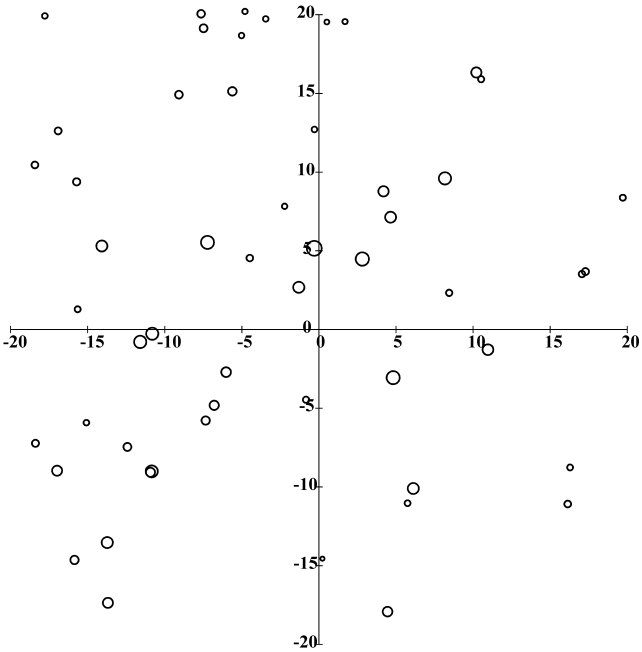

Figure 1 – Photographic radiants centered at the MK-49 radiant. Circle radii mean the orbital similarity with MK-49: azimuthal equidistant projection in ecliptic coordinates. The line λ–$\lambda_{\odot}$=130°.4 runs along the y-axis and axes are labeled in degrees.

Terentjeva (1966) concluded that several photographic meteors some of which are included in MK-49 are Winneckids but many other investigators, for example, Lindblad (1971), insisted they are related to 73P/Schwassmann-Wachmann 3. We had better examine the condition of the meteor activity around them.

There is no reliable radiant associated with both showers in Denning's catalogue (Denning, 1899). This seems to be a natural consequence of both comets chang-

[1]The Nippon Meteor Society (NMS), 4-3-5 Annaka, Annaka-shi, Gunma-ken, 379-0116 Japan. Email: geh04301@nifty.ne.jp

IMO bibcode WGN-431-koseki-recurrent
NASA-ADS bibcode 2015JIMO...43...14K

Table 1 – Photographic meteor showers of Koseki by cluster analysis (converted from B1950 as shown in Koseki (1982; 1986; 2009) to J2000).

MK-No.	Month	Day	α	δ	λ–$\lambda_\odot$	β	V_g	e	q	i	ω	Ω	$\lambda_\odot$	N
49	6	7.11	229.2	40.5	130.4	55.2	14.8	0.628	0.979	19.1	201.2	76.5	76.5	18

Table 2 – Visual radiants possibly originating from 73P/Schwassmann-Wachmann 3 (Koseki, 1978; 1979; 1980; 2009; B1950).

Reference	No.	$\lambda_\odot$	α	δ	λ–$\lambda_\odot$	β	Obs.
NMS	13	81	253	35	164	56	24
AMS	24	60	240	29	170	48	9
Hoffmeister	21	64	249	39	172	59	20
Mean		68	247	34	169	54	

Table 3 – Visual radiants possibly related to 'Winneckids' (Koseki, 1978; 1979; 1980; 2009; B1950).

Reference	No.	$\lambda_\odot$	α	δ	λ–$\lambda_\odot$	β	Obs.
NMS	16	93	217	54	86	61	9
AMS	39	99	224	55	83	65	16
Hoffmeister	36	96	218	52	86	60	11
Mean		96	220	54	85	62	

ing their orbits and their meteoroids encountering the Earth later. Visual observations of the early 20th century caught the apparition of both activities (Tables 2 and 3) but not in the latter half of that century.

Figure 2 shows the recent video radiants' distribution with meteor showers known well. The author compiled the reference list of the meteor showers (Koseki, 1981; 2009) and found the two combinations listed in Table 4 may relate to the two meteor showers Winneckids and meteors of 73P/Schwassmann-Wachmann. Ref-No. 67 includes L1-168 which is identical with IAU-61 (IAUMDC, 2013; Table 5) and seems to be the meteor shower of 73P/Schwassmann-Wachmann. But, it includes also T1-90 which Terentjeva indicated as Winneckids. The other three showers, T1-76, T1-78, and T1-80 are widely spread in appearance because they were detected by the geobased research and are united by the orbbased one.

The video radiants do not have a clear center and suggest the radiant might be larger than we imagine, if it exists. It is necessary to note that the 1998 Winneckid photographic radiant (EN-270698=IAU-170, Figure 2 and Table 5) shown as a dashed circle is located within the MK-49 area. Video observations in 2010 marked as triangles might suggest that 'Winneckids' returned in 2010 in succession to the 1998 (Hashimoto & Osada, 1998) and 2004 (Sato, 2004) recurrent events. There are 10 radiants just to the left of IAU-170 but two of them, i.e. radiants of 2007 and 2008, should be rejected because they were recorded far from the dates of the other eight. The average data of the eight are shown in Table 6.

We will start the survey of these two meteor showers MK-49 and 2010 video June Bootids; abbreviated TAH and JBO hereafter. Figure 3 shows the meteor activity

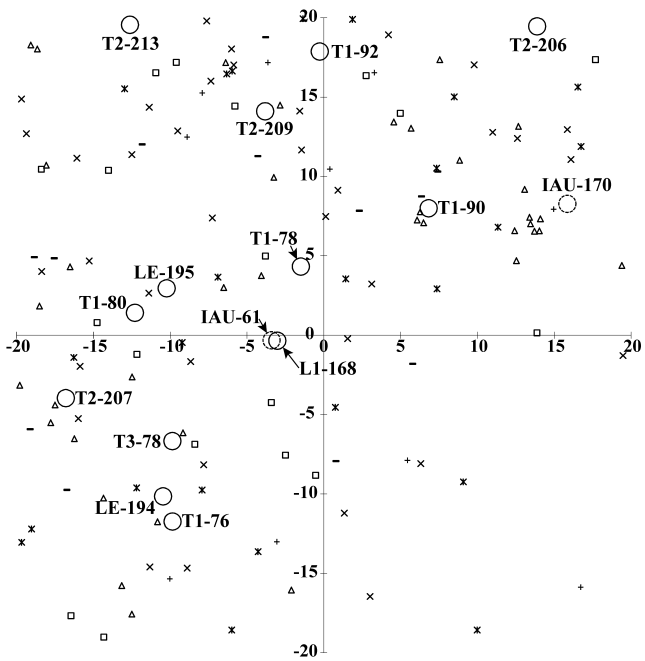

Figure 2 – Video radiants centered at the MK-49 radiant; symbols are the same as in Figure 6 of Paper II (Koseki, 2014b). EN270698 is suggested as a candidate meteor by Jenniskens (2006, p. 337) and corresponds to IAU-170 (JBO). L1-168 corresponds to IAU-61 (TAH).

profiles deduced from the search by the condition of $D(M,N) < 0.30$ for JBO and TAH. It is clear that within the searched boundary exist several components at least and we divide them into four: A; $50 \leq \lambda_\odot < 65°$, B; $65 \leq \lambda_\odot < 76°$, C; $76 \leq \lambda_\odot < 87°$, D; $87 \leq \lambda_\odot < 97°$. It seems other activities might exist there, but they are beyond the limit of our search because we start from the JBO (Table 6) and TAH (Table 1) orbit.

The fluctuations in the profiles suggest the four meteor activities. They are not chance associations by the natural fluctuation in sporadic activities, because both the profiles of photographic and video meteors in Figure 3 are in good agreement. All four sets (Table 7) are in good agreement, though the average data of divisions A and D from photographic meteors may have a large error because of the scarcity of meteors. We will use four video data sets, A(S,T), B(S,T), C(S,J), and D(S,J) as the representatives of the four and abbreviate them AS, BS, CS, and DS respectively. It is necessary to note these data sets are the preliminary ones, because they are divided by the dip in the profiles, i.e. the frequency of meteors.

59 meteors belong to AS and it is the most distinct activity of the four. Orbital elements are somewhat different from the other three in D-criterion distance. It is interesting that photographic meteors are scarce in this area and that a possible meteor shower of AS has not been detected, although we can find several ra-

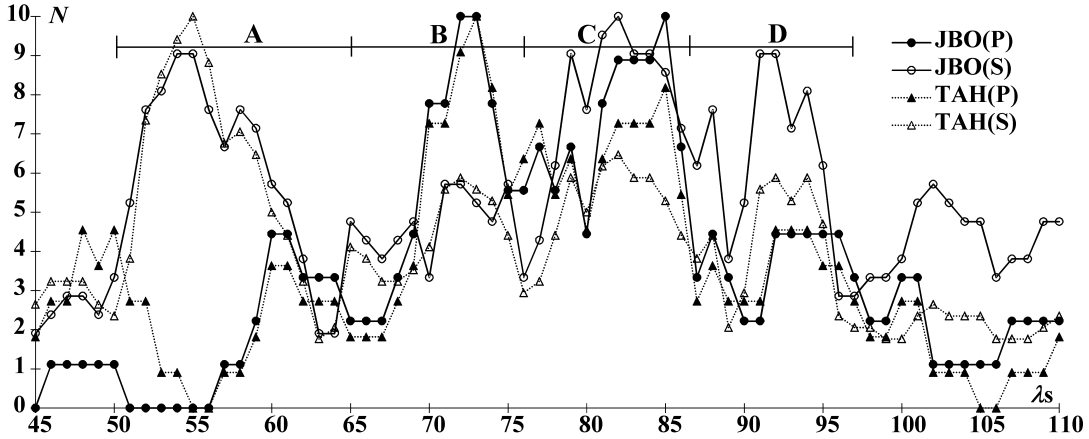

Figure 3 – The meteor activity profiles of JBO and TAH. The line JBO(P) is the 5° in $\lambda_\odot$ moving mean of the meteor numbers searched in the photographic meteors database by the orbit of JBO. JBO(S): searched in SonotaCo data 2007–2012 by JBO. TAH(P): searched in photographic meteors by TAH. TAH(S): searched in SonotaCo data by TAH. Each profile is normalized to have the maximum number as 10.

diants possibly related to AS in visual observations of Denning's, Hoffmeister's, AMS', and NMS', albeit they are much dispersed (see Paper I for further description of these observing data sets). If we search possible AS meteors with the condition $D(M,N) < 0.20$ in video meteors, the candidates are still well dispersed on the celestial sphere like visual ones. AS is so dispersed in radiant that it is hard to perceive AS by the geobased search though the activity is certain as shown in Figure 3. We refine AS by the condition $D(M,N) < 0.20$ and $50 \leq \lambda_\odot < 65°$ and the result is shown in Table 8.

Former photographic MK-49 members are distributed widely from AS beyond DS, though the main part of them are in BS or CS. The orbits of BS and CS are so close that we can unite them into one stream, but there are clear dips in the profile of both photographic and video around $\lambda_\odot$=76° (Figure 3). The search starting from BS makes the scene unclear, but if we use the B(P,T) as the initial data and search in photographic data, the component B is clear and exceeds the component C. If we start from CS, we confirm the activity of the component C and do not recognize BS activity. It seems that the component B was active in the past photographic observations and the component C has been continuing to be active in both video and photographic meteors. The best data for the components B and C are shown in Table 8 by refining with the condition $D(M,N) < 0.20$ and the division by $\lambda_\odot$ shown above; CP by photo and CS by video.

Though the photographic meteors do not show the peak around $\lambda_\odot$=92°, the narrow but sharp one is very clear in video data. But it is on the broad outskirts of CS and so it is proper to use the former JBO (Table 6) as the best data.

Their radiants are largely dispersed but their orbits seem to be closely related. Table 9 shows the $D(M,N)$ matrix on their orbits with the possibly related comets (Table 10). Because CS and CP are identical, their $D(M,N) = 0.041$ means such a small difference could be accepted as due to observational errors. It is clear that the components B–D are so closely related that one can say they are one, though the component A is close enough to the component B; $D(M,N) = 0.131$ is smaller than $D(M,N) = 0.153$ between KCG1 and KCG2 (see Paper II).

If we choose the recent orbit of 73P/Schwassmann-Wachmann 3-C instead of 1930 VI, the distance between the comet and the component A becomes $D(M,N) = 0.098$ though those of the other components increase. It might be suggested the component A comes from a recent ejection from 73P/Schwassmann-Wachmann 3 and the components B–C are the past traces of the comet.

In the case of JBO the situation is very complex, because the distance between 7P/Pons-Winnecke and JBO is not less than $D(M,N) < 0.10$ though the motion of the dust trail confirmed the relationship (Sato,

Table 4 – Two meteor shower groups recognized by cluster analysis with condition $D(M,N) < 0.15$. Abbreviations used here are the same as in Table 5 of Koseki (2009) and the elements are converted from B1950 to J2000.

Ref-No.	α	δ	λ–$\lambda_\odot$	β	V_g	e	q	i	ω	Ω	$\lambda_\odot$	
67	230.4	39.3	136.0	54.8	15.7	0.634	0.974	19.3	204.1	74.2	74.3	T1-76, T1-78, T1-80, T1-90, L1-168
87	245.5	68.6	60.6	80.5	19.9	0.610	1.012	31.7	173.1	95.2	95.2	T1-91, S2-44

Table 5 – Meteor showers listed by IAUMDC in studied area.

IAU-No.	α	δ	λ–$\lambda_\odot$	β	V_g	e	q	i	ω	Ω	$\lambda_\odot$	
61	228.5	39.8	136.2	54.7	15	0.640	0.97	18.6	204.2	72.6	72	τ-Herculids
170	222.9	47.9	97.8	59.6	14.1						96.3	June Bootids

2004). We had better realize the limitation of the meteor shower research – its purpose is to seek the meteor showers, not to hunt for the parents. The question remains whether 7P/Pons-Winnecke may be related to the components B and C. This question should be answered by tracing back their orbits.

Radar surveys, both Harvard and CMOR, could not detect either shower. Past photographic and recent video meteors are brighter meteors due to larger meteoroids than those which radar can detect. The above mentioned four components of the June Bootid Complex are of slow meteors and the efficiency of radiation is very low in such meteors. We miss slower meteors compared to faster ones even if their mass is equal by reason of the velocity and it is true especially in radar observations as a matter of course.

We cannot observe these two cometary showers well at present because of their orbital situation. Firstly, their intersection condition with the Earth is becoming worse at the present time and, secondly, their slower velocity decreases our perception of their meteors. But, we will eventually detect them by some technique because of their recurrent nature.

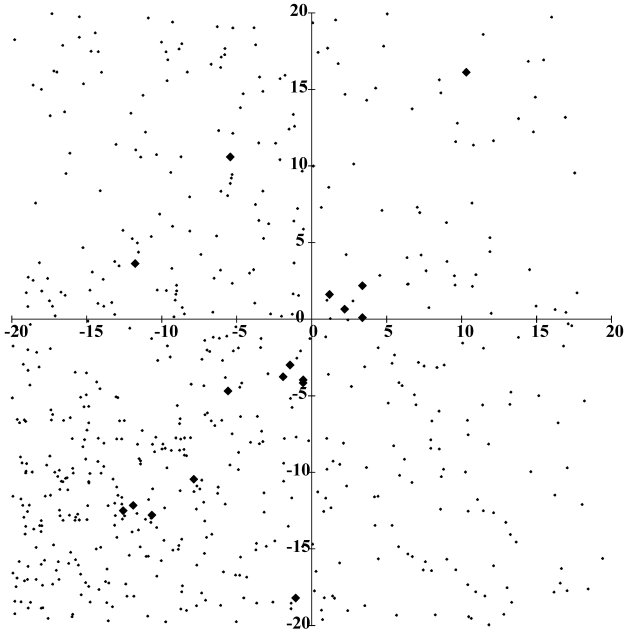

Figure 4 – Distribution of photographic meteors $D(M,N) < 0.20$ from MK-127 shown with black diamonds and meteors all the year round with small black circles.

2 'Bielids' and 'Andromedids'

The spectacular meteor storms on November 27, in 1872 and in 1885, are well known. The Andromedids then became weaker and weaker and were thought to be lost now. Hawkins et al. (1959) reported the recovery of it in Super-Schmidt meteors and suggested the radiant point and the activity period moved. The author also searched the traces of the Andromedids in the photographic meteor database and found the identical set (Table 11; Koseki, 1982).

Figure 4 is centered at the MK-127 radiant in (λ–$\lambda_\odot$, β) coordinates and shows the photographic radiants within $D(M,N) < 0.20$ from MK-127 and surrounding radiants $D(M,N) \geq 0.20$ observed in this area the whole year round. Firstly, it is impressive the probable candidates of Andromedids are distributed along the line stretching through the center to upper right. This distribution will be confirmed below by video observations. Secondly, ANT (the antihelion source) is clearly represented towards the lower left and the line of Andromedids candidates links up to ANT.

The author compiled the reference list of published meteor showers by using cluster analysis and found two streams (three showers) have a close relation with Andromedids (Table 12). Ref-No. 11 and 197 constitute one stream, in other words, the twin. L1-129 is listed (by the original author) as a-Triangulids but is clearly identical with MK-127 and LE-630 is designated as Andromedids by the authors. There are three meteor streams excluded by the cluster analysis yet needing consideration (Table 13).

Radar radiants recorded by the Harvard projects do not show clear evidence of Andromedids activity (Figure 5), though S1-9 is listed as Andromedids. S1-9 lies

Table 6 – June Bootids recorded by video observations in 2010.

Source	Month	Day	α	δ	λ–$\lambda_\odot$	β	V_g	e	q	i	ω	Ω	$\lambda_\odot$	N
SonotaCo	6	24.73	224.0	47.2	103.4	59.4	14.0	0.675	1.014	18.5	185.9	92.6	92.6	8

Table 7 – The four divisions detected from the profiles (Figure 3). A–D are the divisions indicated in Figure 3. The searched data is shown first in the parentheses and the base orbit second; B(P,T) means the data of the division B obtained in photographic meteors by the orbit of TAH, C(S,J) is the division C of SonotaCo meteors by JBO and so on.

Division	Month	Day	α	δ	λ–$\lambda_\odot$	β	V_g	e	q	i	ω	Ω	$\lambda_\odot$	N
A(P,T)	5	19.49	219.2	23.2	149.2	36.2	14.8	0.662	0.921	14.3	218.5	58.9	58.9	5
A(S,T)	5	17.41	220.6	27.8	150.5	40.7	15.2	0.632	0.929	16.0	216.8	56.0	56.0	59
B(P,T)	6	1.54	229.2	33.0	142.6	48.5	14.7	0.621	0.965	17.7	208.6	71.0	71.1	13
B(S,T)	6	1.21	227.0	35.2	136.5	49.2	14.7	0.615	0.966	17.5	205.3	70.3	70.3	33
C(P,J)	6	12.27	234.1	45.5	123.1	60.5	15.7	0.629	0.993	21.5	195.5	81.7	81.7	15
C(S,J)	6	13.01	230.6	41.5	126.4	56.0	14.8	0.628	0.991	19.3	197.2	81.6	81.6	39
D(P,J)	6	23.56	229.5	43.3	108.4	55.9	14.7	0.612	0.999	19.6	188.8	92.3	92.3	7
D(S,J)	6	23.81	227.8	47.4	106.0	60.3	14.6	0.651	1.009	19.6	187.0	91.8	91.8	24

Table 8 – The most plausible data for the four components of June Bootid Complex.

Division	Month	Day	α	δ	λ–$\lambda_\odot$	β	V_g	e	q	i	ω	Ω	$\lambda_\odot$	N
A	5	17.20	217.2	27.1	147.6	39.0	14.7	0.645	0.936	14.6	215.4	55.7	55.7	40
B	6	1.41	230.1	36.0	142.0	51.6	14.9	0.621	0.970	18.5	207.3	70.9	70.9	11
CP	6	11.67	229.7	42.4	122.9	56.9	14.0	0.607	0.996	18.5	196.3	81.1	81.1	10
CS	6	13.03	231.1	41.1	127.8	56.3	14.7	0.636	0.991	19.2	198.1	81.6	81.6	24
D=JBO	6	24.73	224.0	47.2	103.4	59.4	14.0	0.675	1.014	18.5	185.9	92.6	92.6	8

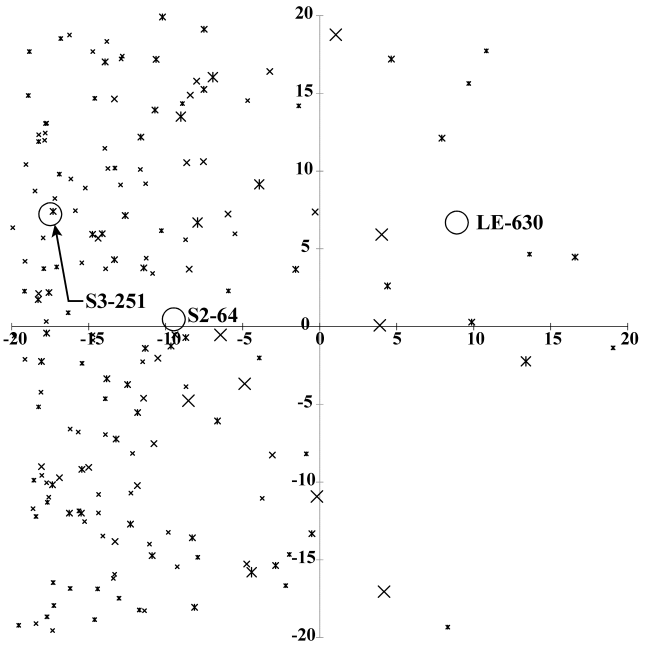

Figure 5 – Radar radiant distributions of meteors in the region around MK-127 having $D(M,N) < 0.3$ from MK-127, with remaining meteors in $220 \leq \lambda_\odot < 260°$ also shown. Asterisks for 1961–65 and crosses for 1968–69 observations. The largest marks represent $D(M,N) < 0.2$, that is, probable Andromedids; the smaller ones $0.2 \leq D(M,N) < 0.3$, that is, possible ones; and the smallest $D(M,N) \geq 0.3$ the remainder. Circles are radar meteor showers shown in Tables 12 and 13.

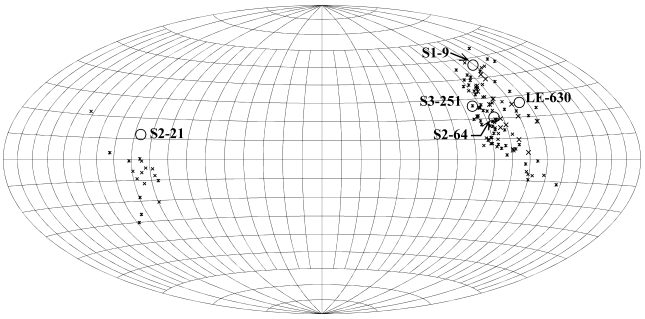

Figure 6 – Hammer projection view of Harvard radar meteors having $D(M,N) < 0.3$ from MK-127.

above the top of Figure 5 and the activity period of S1-9 does not coincide with the video observations (see below). MK-127 is more similar to S2-64 (Triangulids) rather than S1-9. Sekanina started searching from the orbit of P/Biela in the 19th century and the result is settled at S1-9. It is, however, very interesting CMOR's observations reported 'Andromedids' outbursts in early December 2011 and 2013 (Spaceweather, 2013).

It is worth noticing he pointed out S2-64 has its twin S2-21 (χ-Piscids) as the daytime shower. Radiants of $0.2 \leq D(M,N) < 0.3$ in the 3rd quadrant of Figure 6 may be the precursors of future Bielids, if its orbital node rotates as indicated by former studies (see below).

A video Andromedids search starting from MK-127 shows us very important views in its orbital evolution. Firstly, Figure 7 shows the video meteor profile and the estimated number of meteors calculated from the author's method (Koseki, 2012a). The peak of the observed rates is reached about $3.^\circ5$ earlier in $\lambda_\odot$ than the estimated one that is based on observations around the 1950's. Video observations used here have been carried out in 2007–12 and the regression of the node is $3.^\circ5$

Table 9 – The $D(M,N)$ matrix for the four components of June Bootid Complex with their possibly related comets.

	1930 VI	1921 III	A	B	CP	CS
1930 VI						
1921 III	0.125					
A	0.142	0.254				
B	0.123	0.217	0.131			
CP	0.107	0.168	0.169	0.066		
CS	0.122	0.178	0.183	0.068	0.041	
JBO	0.122	0.120	0.220	0.139	0.096	0.081

Table 10 – Orbits of the two comets. *JPL (2014). #Marsden (1989), converted from B1950.0 to J2000.0.

Comet	e	q	i	ω	Ω	a	Q	P
1930 VI #	0.6718	1.0114	17.39	192.35	77.73			5.41
73P/Schwassmann-Wachmann 3-C*	0.6922	0.9429	11.38	198.87	69.84	3.063	5.184	5.36
1921 III #	0.6855	1.0409	18.92	170.30	99.20			6.02
7P/Pons-Winnecke*	0.6374	1.2411	22.34	172.40	93.43	3.422	5.604	6.33

Table 11 – Photographic meteor showers by Koseki using cluster analysis (converted from B1950 as shown in Koseki (1982; 2009) to J2000) comparing with IAU-18 (AND).

Source	Month	Day	α	δ	λ–$\lambda_\odot$	β	V_g	e	q	i	ω	Ω	$\lambda_\odot$	N
MK-127	11	8.97	21.7	31.2	164.9	20.5	18.2	0.755	0.774	10.4	240.5	227.2	227.2	9
IAU-18			24.2	32.5	162.6	20.8	17.2	0.714	0.789	10.0	238.9	231.0	232.0	18

Table 12 – Two meteor streams recognized by the cluster analysis with condition $D(M, N) < 0.15$. Ref-No. 11 and 197 are twin showers. Abbreviations used here are the same as in Table 5 of Koseki (2009) and the elements are converted from B1950 to J2000.

Ref-No.	α	δ	λ–$\lambda_\odot$	β	V_g	e	q	i	ω	Ω	$\lambda_\odot$	
187	28.8	33.2	161.0	20.0	20.3	0.745	0.807	9.3	234.8	237.9	237.9	LE-565, LE-630, LE-631, LE-632, L1-129
11	19.2	21.1	6.6	12.0	18.0	0.672	0.696	6.6	103.9	19.1	19.1	S2-21
197	44.6	7.4	161.8	−9.1	19.4	0.691	0.762	5.0	73.3	48.0	242.6	LE-633, LE-635

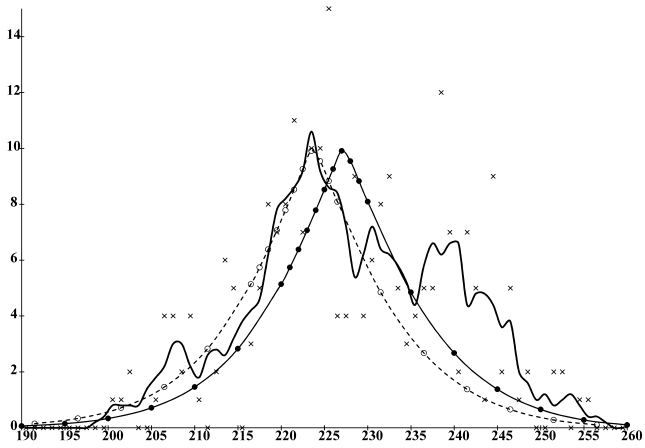

Figure 7 – The profile of video Andromedids selected with $D(M, N) < 0.20$ from MK-127 and the estimation by the simple model (Koseki, 2012a). Crosses are the raw number of Andromedids for 2007–12 and the solid line is the moving mean using 5° bins in $\lambda_\odot$. The solid line with black circles is the estimated profile of Andromedids based on MK-127 and the dashed line with open circles is the shifted estimation by $\Delta\lambda_\odot = 3.^\circ5$ from MK-127.

in some 50–60 years. The difference between photographic observations and video is 56 years on average and the regression rate may be $6.^\circ2$/century. The regression of the node does not mean the rotation of the orbital axis but the node itself rotates around the ecliptic pole similar to the precession of Earth. This orbital evolution makes meteor shower twins and Andromedids might have its twin as a daytime shower (χ-Piscids) in future.

If we shift the estimated line to the left by $3.^\circ5$ in $\lambda_\odot$, the estimation (the dashed line in Figure 7) is in accordance with the observations satisfactorily. Whether the deviations of the observations from the estimation come from the fluctuations of the sporadic background or the smaller peak of Andromedids itself is unclear because the amount of observations is not enough yet. The photographic radiant distribution (Figure 4) suggests the ANT activity, such as the Taurid complex, veils the Andromedids and the video profile (Figure 7), on the other hand, suggests Andromedid activity fluctuates after the maximum.

Secondly, Figure 8a–f show the video radiant distributions around MK-127 along solar longitude from $\lambda_\odot = 220^\circ$ to $\lambda_\odot = 250^\circ$. It is noticeable the small radiant crowd moves from center to upper right and this is suggestive of the elongated distribution of the photographic radiants. The crowd of radiants passes through the 1872 Andromedid storm around $\lambda_\odot = 245^\circ$. We can converge to a solution for the radiant as a function of $\lambda_\odot$ starting from this small crowd of radiants with the radiant radius $r < 3^\circ$, excluding $\lambda_\odot < 220^\circ$ meteors in order to avoid ANT contaminations. Figure 9 and Table 14 show the results. Table 14 gives the extrapolation to the earlier activity period excluded in the convergent process but makes clear the difficulties discriminating from ANT activities. This radiant crowd moves almost along the declination, that is, does not drift eastward but northward.

This radiant movement represents the Bielids' orbital evolution. We selected 70 meteors in total as tracing the Bielids according to the converged solution. Their orbital elements and geocentric velocity change clearly with $\lambda_\odot$ and they suggest the genetic relation to 3D/Biela (Tables 15 and 16).

3 Meteor showers in radar observations

Radar meteor showers are fewer in the whole IAU list than video ones, though recent CMOR showers (Brown et al., 2008; 2010) arouse our interest. Past radar show-

Table 13 – Rejected by the cluster search but interesting showers. Abbreviations used here are the same ones (Table 5 of (Koseki, 2009)) and shower names are given by the original authors.

Source	α	δ	λ–$\lambda_\odot$	β	V_g	e	q	i	ω	Ω	$\lambda_\odot$	Stream
S1-9	12.0	57.1	161.0	46.5	18.5	0.708	0.863	21.5	225.8	238.5	238.5	Andromedids
S2-64	35.2	35.8	175.0	20.6	20.3	0.724	0.676	12.7	255.8	229.9	229.9	Triangulids
S3-251	31.2	40.9	184.5	26.5	21.1	0.647	0.606	18.3	269.6	219.3	219.3	Triangulids

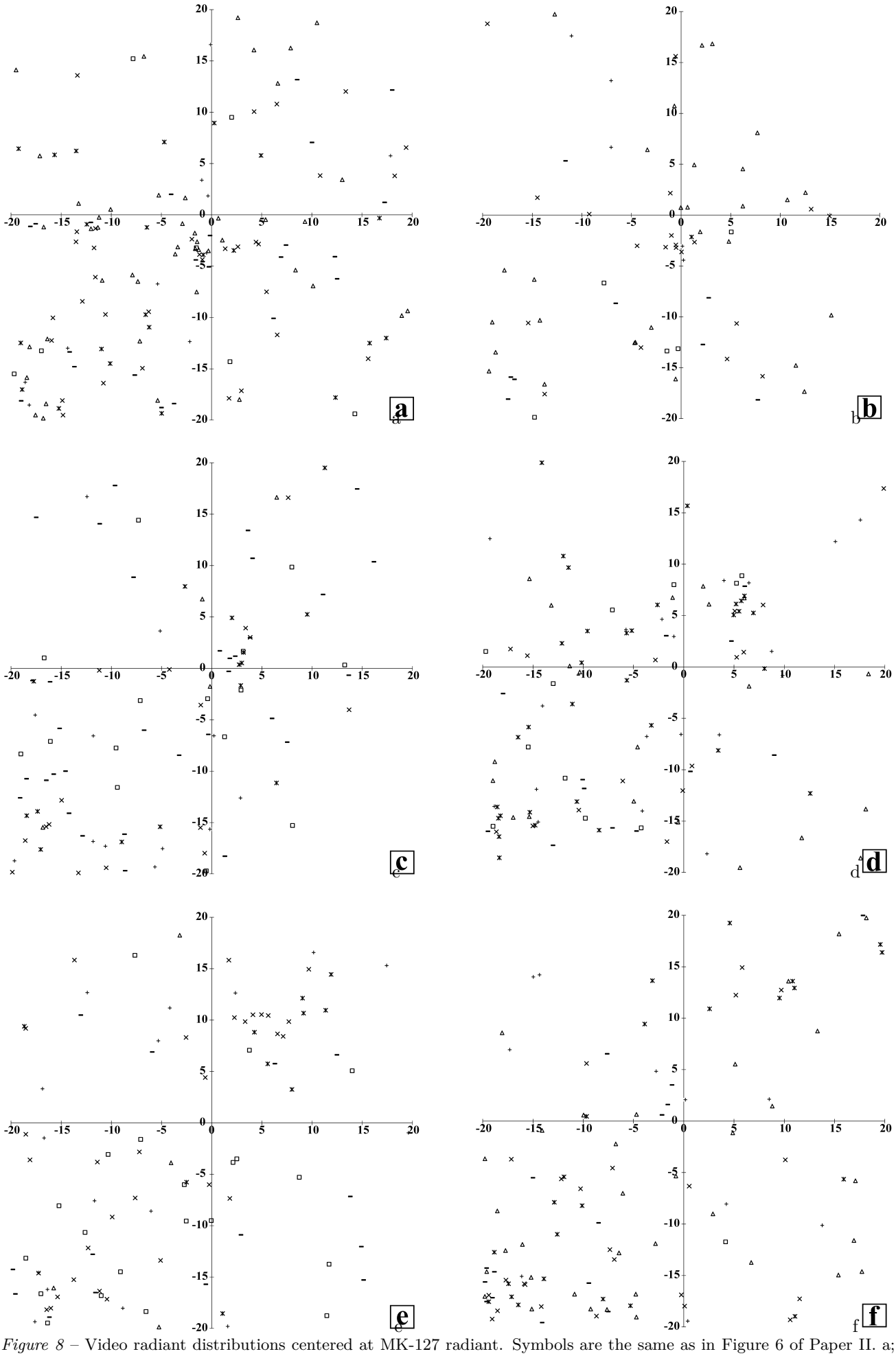

Figure 8 – Video radiant distributions centered at MK-127 radiant. Symbols are the same as in Figure 6 of Paper II. a; $220 \leq \lambda_{\odot} < 225$, b; $225 \leq \lambda_{\odot} < 230$, c; $230 \leq \lambda_{\odot} < 235$, d; $235 \leq \lambda_{\odot} < 240$, e; $240 \leq \lambda_{\odot} < 245$, f; $245 \leq \lambda_{\odot} < 250$.

Table 14 – The radiant drift of Andromedids suggested by video observations.

$\lambda_\odot$	210	215	220	225	230	235	240	245	250	255	260
α	17.7	18.9	20.1	21.2	22.2	23.0	23.6	24.0	24.1	23.7	22.9
δ	15.4	19.7	24.0	28.1	32.3	36.3	40.1	43.9	47.5	50.9	54.0
λ–$\lambda_\odot$	172.2	169.9	167.6	165.3	162.8	160.2	157.5	154.6	151.5	148.1	144.5
β	7.3	10.9	14.4	17.8	21.3	24.7	28.0	31.3	34.5	37.6	40.7

Table 15 – The orbital elements by the least squares solution strongly indicate recent Andromedids are the descendants of Bielids.

$\lambda_\odot$	210	215	220	225	230	235	240	245	250	255	260
V_g	20.8	19.9	19.1	18.3	17.5	16.7	15.8	15.0	14.2	13.4	12.5
e	0.826	0.806	0.786	0.767	0.747	0.727	0.707	0.688	0.668	0.648	0.629
q	0.687	0.713	0.740	0.766	0.793	0.819	0.846	0.872	0.899	0.925	0.952
i	6.8	7.6	8.4	9.2	10.1	10.9	11.7	12.6	13.4	14.2	15.0
ω	254.2	250.1	245.9	241.7	237.5	233.3	229.1	224.9	220.7	216.5	212.3

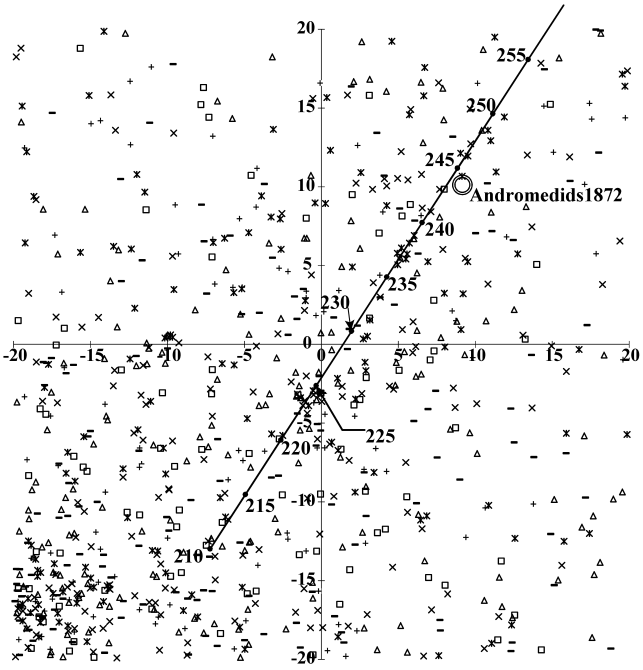

Figure 9 – Video radiant distributions centered at MK-127 radiant with the radiant drift.

Table 16 – Orbital elements of 3D/Biela; Marsden (1989), converted from B1950.0 to J2000.0.

Comet	e	q	i	ω	Ω	P
1772	0.7259	0.9904	17.05	213.34	260.94	6.87
1806 I	0.7459	0.9072	13.59	218.08	254.08	6.74
1826 I	0.7466	0.9024	13.56	218.26	253.98	6.72
1832 III	0.7513	0.8791	13.22	221.66	250.67	6.65
1846 II	0.7566	0.8564	12.58	223.06	248.14	6.60
1852 III	0.7558	0.8606	12.55	223.19	248.01	6.62

ers mostly are not recognized now by video observations as mentioned before. Firstly, radar and video see different magnitude ranges and the difference in magnitude distribution causes the different view (see Paper I). Secondly, half a century passed from former radar observations till video ones, meteor activities changed in many cases (see 'Bielids' for an example), and old showers may have ceased. Thirdly, the conception and the perception of a meteor shower differ from one observer/researcher to another – someone says it can be seen clearly but others say none.

It is worth investigating some CMOR showers as examples, because we can compare them with former radar observations to test the change over many years, with video observations to check the difference in magnitude, and with photographic ones to understand the difference in the conception and the perception. We select three CMOR showers (Table 17) because of their abundant orbits or of the interesting report.

3.1 PPS: IAU-372

CMOR listed the duration of PPS (ϕ-Piscids) as $\lambda_\odot$ = 104–107°, when the Harvard surveys were mainly in interruption, and during the rainy season in Japan. If we survey PPS in other observations for the given duration, we cannot find out its activity. It is proper to search PPS by using the D-criterion for video meteors at first. There are 17 meteors within $D(M,N) < 0.20$ and their average solar longitude is somewhat different, $\lambda_\odot = 111\,^\circ\!.0$ with standard deviation $9\,^\circ\!.6$. It seems to be reasonable to widen the search boundary to $\lambda_\odot$ = $101\,^\circ\!.4$–$120\,^\circ\!.6$. Figure 10 shows the radiant distribution of video meteors centered at (λ–$\lambda_\odot$, β) = ($281\,^\circ\!.7$, $14\,^\circ\!.5$) in this period. It is clear that so many showers, in which radar ones occupy the great majority, have been recorded in this area, because PPS is very near the apex. In Figure 10 video radiants are spread towards the upper right from the center and there are four showers (Table 18) within the concentration. The last line of Table 18 shows the average of video meteors within $r < 5°$ at (λ–$\lambda_\odot$, β) = (280°, 16°). These meteor showers including PPS locate near the apex and the small difference in radiant point or in velocity causes very large discrepancies in orbital elements. If we took the contamination from the apex source into consideration, the apparent difference in the geocentric velocity is much smaller, indicating they are one stream. Though the abundant meteors from the apex source make a clear discrimination almost impossible, the existence of these activities is suggestive of the longer and later PPS activity period.

Table 17 – Three CMOR showers selected for this investigation.

IAU	code	α	δ	λ–$\lambda_\odot$	β	V_g	e	q	i	ω	Ω	$\lambda_\odot$	N
372	PPS	20.1	24.1	281.7	14.5	62.9	0.590	0.8559	152.6	125.02	106	104–107	1395
388	CTA	63.2	24.7	205.8	3.5	42.1	0.984	0.0807	12.3	328.49	220	194–227	1850
404	GUM	231.8	66.8	222.5	75.1	31.8	0.772	0.9593	51.1	199.54	299	294–304	694

Table 18 – Possible candidates related to PPS.

Code	Month	Day	α	δ	λ–$\lambda_\odot$	β	V_g	e	q	i	ω	Ω	$\lambda_\odot$	N
IAU-414			28.9	28.1	276.8	15.2	71						120	192
LE-292	7	18–22	27.5	27.5	276.8	15.2	56.4	0.24	0.74	148.8	65.8	118.6	118.6	9
LE-293	7	17–22	28.5	30.8	279.4	17.9	63.8	0.59	0.92	146.8	137.9	118.2	118.2	10
T3-88	7	20–30	28.9	32.3	279.3	19.1	61.1	0.492	0.91	144.1	133.0	119.1	119.1	
SonotaCo	7	15.36	24.4	27.3	280.4	16.0	66.4	0.859	0.915	151.2	141.8	112.3	112.3	123

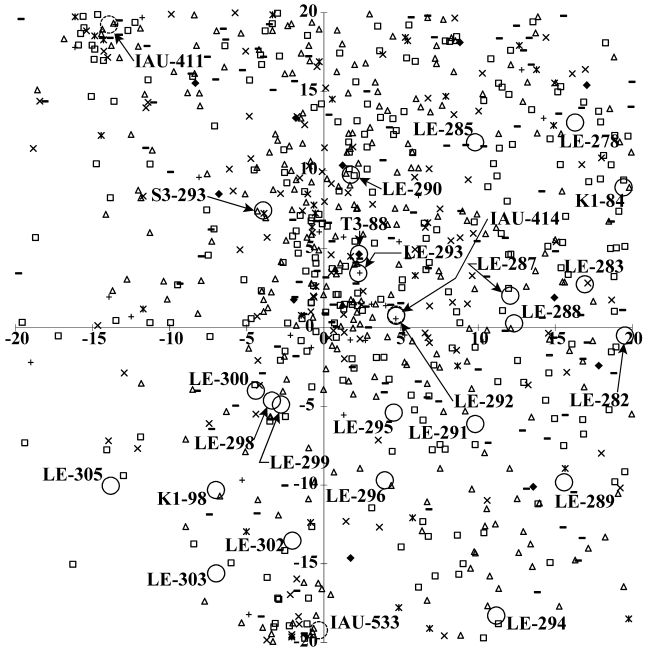

Figure 10 – The distribution of radiants around PPS; black diamonds represent photographic ones and others are video shown by the same symbols as in Figure 8.

3.2 CTA: IAU-388

CTA (χ-Taurids) is near the Taurid complex and ANT. Visual observations recorded several radiants near CTA but they are almost buried under Taurids and ANT. Photographic and II (Image Intensifier) meteors do not indicate CTA activity (Figure 11a) and show a similar environment as visual observations. Radar radiants from the Harvard surveys seem to suggest a concentration (Figure 11b) around the CTA region, but they may come from S3-257 or other radar showers (see Table 19). Meteor showers shown in Figure 11b labeled with a reference are radar ones except for IAU-417 (ETT) and suggest the activity of faint meteors. But recent video radiants seem to concentrate around CTA also (Figure 11c) and suggest the activity of bright meteors in recent years. It is necessary to note these figures are drawn assuming a long duration for CTA, as taken from CMOR data.

Searching in video meteors with the condition (λ–$\lambda_\odot$, β) = (206°, 6°), that is the center of video radiants in Figure 11c, and $r < 5°$, we can get the probable CTA activity in this long period. Figure 12 shows the profile of the meteor numbers in moving mean 5° bins in $\lambda_\odot$ and confirms CTA is under the strong influence of the Taurid complex. The author suggested Taurids consist of three components; S_E, S_F, and northern branch (Koseki, 2012b). The profile of CTA obtained by video observations indicates the maximum occurs at $\lambda_\odot = 223°$ when the northern branch reaches its peak while S_F is active and then this becomes the richest period of total Taurid activity. The secondary peak of CTA at $\lambda_\odot = 205°$ coincides with the maximum of S_E activity.

The profile estimated in the same way as for the Andromedids implies the CTA duration published in the CMOR list seems to be too long during the first part of the shower and too short for the later part. That is, the contaminations from Taurids and ANT are estimated as about 4 meteors in Figure 12, so that the period of CTA activity recognizable above the sporadic background starts at $\lambda_\odot = 213°$ and ends at $\lambda_\odot = 230°$, though the CMOR duration is $\lambda_\odot = 194$–$227°$. CTA may have been active before the 1960's when visual and

Table 19 – Possibly related showers to CTA.

Code	Month	Day	α	δ	λ–$\lambda_\odot$	β	V_g	e	q	i	ω	Ω	$\lambda_\odot$	N
K1-147	9	21–28	42.7	20.2	207.6	3.7	43	0.98	0.07	16.0	332.0	198.7	198.7	83
IAU-417			55.5	23.7	207.7	3.9	47						211	323
LE-524	10	22–27	49.3	24.0	202.2	5.6	41.7	0.98	0.13	15.1	318.8	211.1	211.1	14
LE-528	10	22–27	56.5	22.9	208.1	2.9	43.9	0.98	0.06	12.1	333.8	211.3	211.3	40
NI-61.10.7	10	26–30	59.7	21.3	207.0	0.8	35.2	0.92	0.12	2.4	328.9	215.1	215.0	3
S3-257			67.2	30.4	208.1	8.5	34.2	0.910	0.132	19.6	326.1	222.1	222.1	24

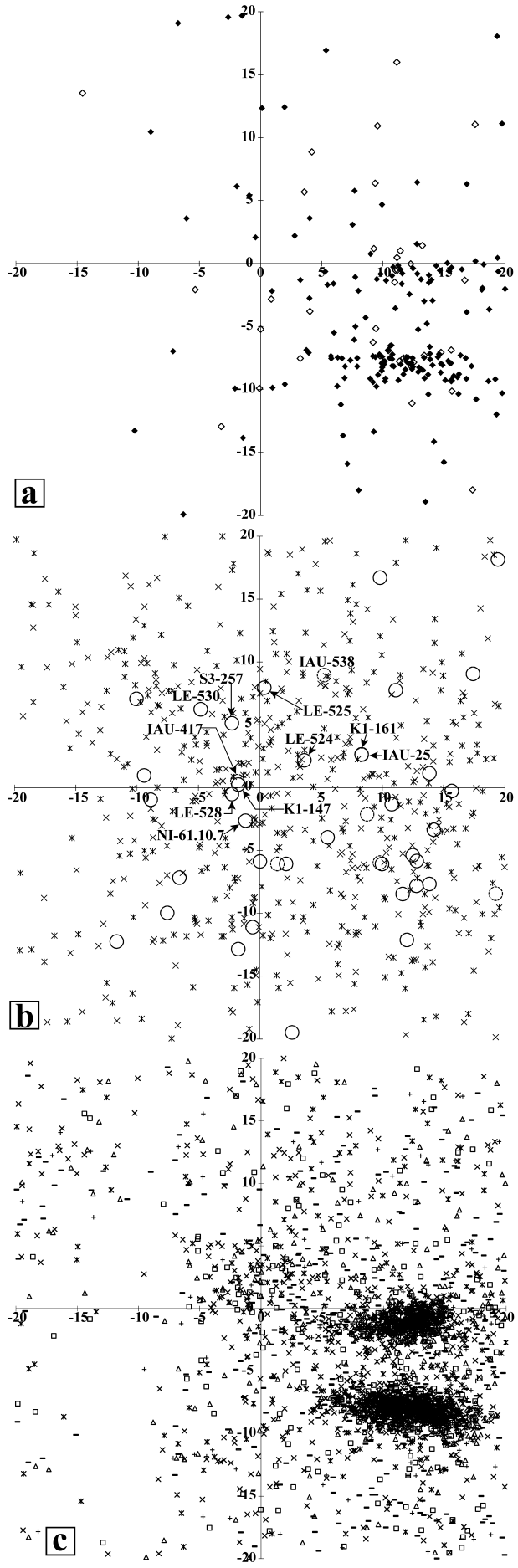

Figure 11 – The radiant distributions around CTA in $\lambda_\odot = 194$–$227°$. a; photographic radiants (black diamond) and II radiants (diamond), b; Harvard radar surveys with the meteor showers, c; SonotaCo video radiants shown by the same symbols as in Figure 8.

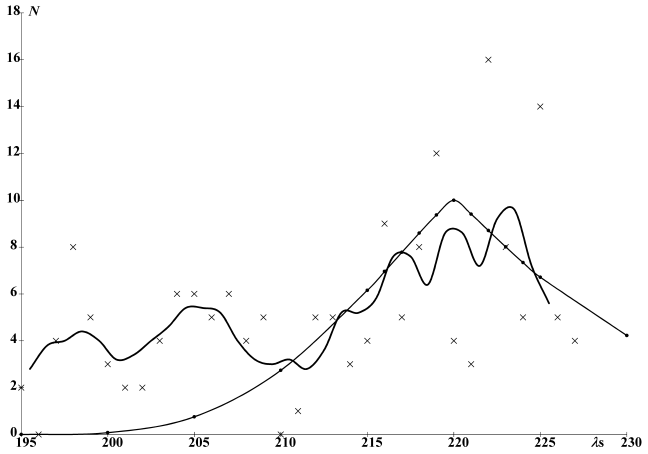

Figure 12 – The video meteor profile for probable activity of CTA. Meteors are selected by the distance $r < 5°$ from $(\lambda - \lambda_\odot, \beta) = (206°, 6°)$. Crosses mean the raw meteor number in each 1° bin in $\lambda_\odot$ and the solid line represents the moving mean using 5° bins. Solid line with the small dots is the estimated profile.

Table 20 – The number of possible GUM meteors recorded by video.

Year	2007	2008	2009	2010	2011	2012	Total
N	1	3	4	12	8	6	34

photographic observations had still been active, because we could not detect them by visual and photographic observations then, based on the perception and the conception of a meteor shower at that time.

3.3 GUM: IAU-404

Jenniskens and Lyytinen reported ten video meteors of GUM (γ-Ursae Minorids) were recorded on the night of January 20/21 by a Finnish network (Figure 13; Spaceweather, 2010). Japanese video observations recorded the sudden rise of GUM (see Figure 14 and Table 20) also in 2010. A search in video meteors with the condition $D(M, N) < 0.20$ for GUM suggests the activity period of GUM might be longer than in CMOR data and the average data are shown in Table 21. On the other hand, we cannot confirm the record of GUM by the former radar observations except for S3-10 (January Draconids) but there is one possible candidate in photographic meteors: H5-1913.

There is no sign of GUM in visual observations. The activity level is not noticeable by visual observers though GUM is rich in bright meteors judging from the existence of video observations. It is also possible that GUM might have a recurrent nature.

4 Meteor showers in II observations

Video observations are carried out by CCD now but by II (Image Intensifier) several years ago. We can record 2nd magnitude meteors by CCD but observe 7th magnitude and fainter meteors by using II. We revealed the observation devices make the results different from each other in Paper I and Koseki et al. (2010) stressed the difference between CCD and II properties.

Table 21 – Possible GUM observations.

Code	Year	Month	Day	α	δ	λ–$\lambda_\odot$	β	V_g	e	q	i	ω	Ω	$\lambda_\odot$
SonotaCo		1	18.81	229.8	67.2	220.9	74.1	30.5	0.702	0.954	49.7	201.5	297.9	287.3–308.6
S3-10				246.1	62.3	255.3	78.9	26.0	0.449	0.979	44.9	185.8	296.0	296.0
H5-1913	1950	1	20.51	238.3	67.4	221.2	77.7	29.6	0.670	0.955	48.3	202.2	300.6	300.6

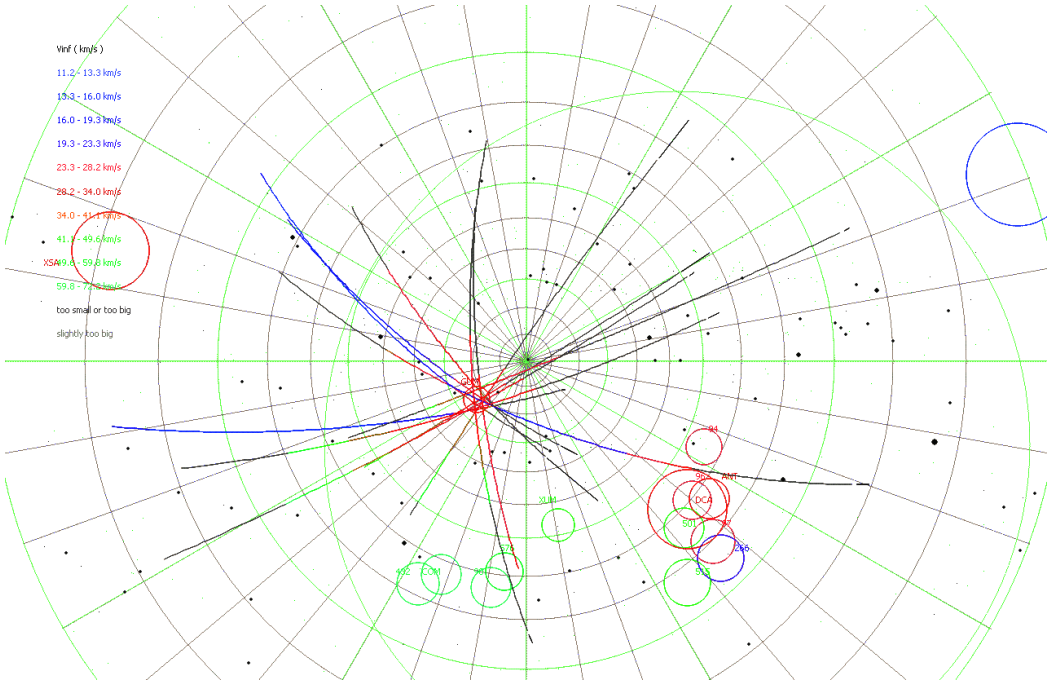

Figure 13 – 2010 GUM observations in Finland. Courtesy Esko Lyytinen.

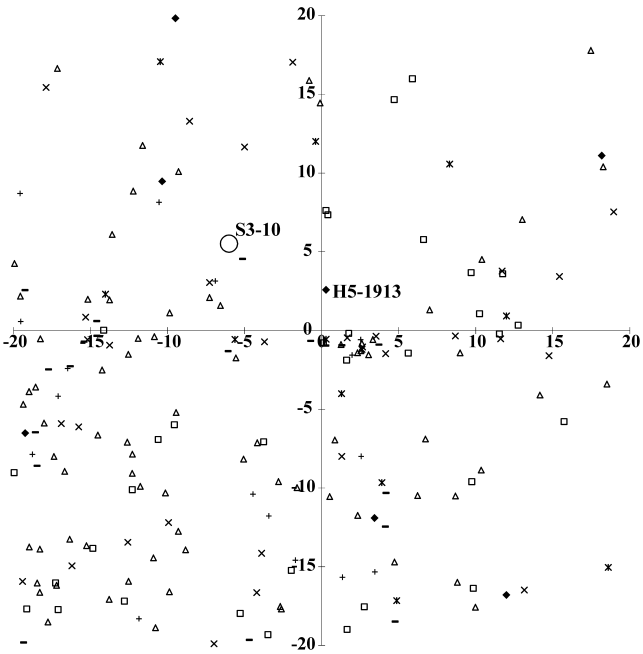

Figure 14 – The video radiant distribution around GUM.

Shigeno & Yamamoto (2012) published a list of 12 new showers by II observations. It is very difficult to confirm these 12 showers by other observations, because they sought radiant condensations excluding published ones. The author reported a precise study on these 12 showers (Koseki, 2013) and found two interesting showers: ETP and ASX (Table 22).

4.1 ETP: IAU-433

ETP (η-Pegasids) was not observed visually except by AMS. AMS-67 in the author's compiled visual radiants (Koseki, 1980; 2009) is located several degrees to the west of ETP near LE-456; $\lambda_\odot = 133\,^\circ\!.1$, $\alpha = 328\,^\circ\!.3$, $\delta = 29\,^\circ\!.3$, $\lambda - \lambda_\odot = 209\,^\circ\!.9$, $\beta = 39\,^\circ\!.0$. There are three radar showers around ETP and one photographic (Figure 15 and Table 23). This represents a characteristic of II observations, because the magnitude range of II observations lies between photographic and radar.

Table 24 shows the 8 photographic meteors around T1-119 and the averages in the lowest line. Though there are three meteors with extremely low geocentric velocity and, therefore, different inclination and argument of perihelion, the averages seem to be identical with ETP. Even if we exclude these three meteors, the average radiant point is about the same. There might be a certain meteor activity, as indicated by II observations, i.e. ETP, but it is necessary to investigate the details in the future. If ETP has recurrent nature, it is possible to explain why ETP is poor in video observations.

4.2 ASX: IAU-439

ASX (α-Sextantids) is observed well by video observations in contrast with ETP. The averages of the meteors enclosed by the ellipse (Figure 16) are shown in Table 25 with NAS (IAU-483). These enclosed radiants do not indicate the drift with the solar longitude and the ellipse represents the radiant area itself. ASX agrees well with

Table 22 – Two II meteor showers of interest.

IAU	code	α	δ	λ–$\lambda_\odot$	β	V_g	e	q	i	ω	Ω	$\lambda_\odot$	$\sigma\lambda_\odot$
433	ETP	334.6	32.7	215.9	39.7	34.5	0.685	0.460	55.1	293.1	134.8	135.40	2.93
439	ASX	154.6	−3.4	280.4	−13.0	68.8	0.947	0.898	155.6	325.3	56.6	237.37	3.60

Table 23 – Showers possibly related to ETP.

Code	Month	Day	α	δ	λ–$\lambda_\odot$	β	V_g	e	q	i	ω	Ω	$\lambda_\odot$	N
T1-119	7/19	8/13	341.7	32.4	217.0	36.7	46.0	0.969	0.467	75.2	274.7	140.8	140.8	
LE-456	8	10–15	332.0	31.8	208.4	40.0	39.7	0.87	0.52	57.8	272.3	139.8	139.8	6
LE-458	8	9–13	338.3	39.5	220.7	44.2	41.6	0.76	0.59	69.4	268.1	138.5	138.5	5
LE-465	8	9–13	346.7	37.6	226.3	39.2	45.7	0.82	0.53	79.9	273.9	139.3	139.3	5

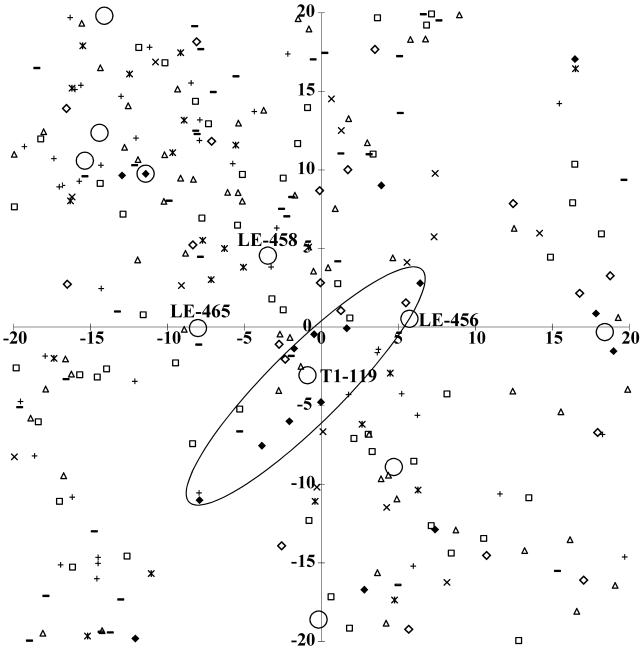

Figure 15 – The radiant distribution around ETP; II meteors (diamond), photographic (black diamond), and video shown by the same symbols as in Figure 8.

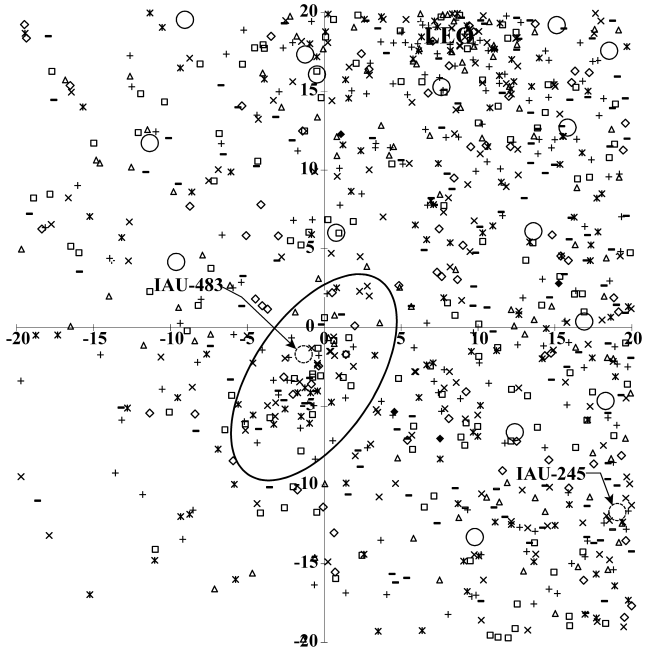

Figure 16 – The video radiant distribution around ASX shown by the same symbols as in Figure 8.

the averages of SonotaCo and with NAS, and therefore NAS should be included in ASX. ASX has been observed by video annually, but both Harvard radar surveys and photographic observations missed it. It is natural that there is no record of ASX in visual observations, because the supposed hourly rates might be too low for visual observers. ASX might have become active in more recent years.

5 General conclusions

1. There are meteor showers observable only by their recurrent events.

Meteor activities are very changeable. Some ceased and others will be born. A meteor shower was very active in the past and it will be unnoticed later. JBO is not only the historical event but recurrent activities have been observed in 1998, 2004, and 2010 possibly. KCG1 seems to be the historical record, KCG2 might

Table 24 – Photographic meteors around T1-119 and possible ETP candidates.

Code	Year	Month	Day	α	δ	λ–$\lambda_\odot$	β	V_g	e	q	i	ω	Ω	$\lambda_\odot$
H1-8472	1953	8	13.25	341.6	34.3	218.2	38.3	45.3	0.940	0.500	75.0	272.0	140.7	140.7
H2-8528	1953	8	13.46	341.9	30.5	215.9	35.0	46.7	0.997	0.433	75.4	277.3	141.0	141.0
D3-620672	1962	8	4.94	333.1	31.5	216.5	39.3	43.8	0.918	0.515	71.6	271.7	132.6	132.6
D4-641561	1964	8	7.70	326.6	32.0	207.2	42.2	36.9	0.842	0.565	55.8	268.2	135.7	135.7
O3-314	1962	8	11.04	345.0	28.7	220.5	32.1	47.5	0.938	0.387	82.6	286.7	138.4	138.4
H1-8159	1953	8	5.23	337.6	27.3	218.4	33.7	14.3	0.450	0.440	20.0	325.0	132.7	132.7
H1-8184	1953	8	5.33	346.6	25.3	224.8	28.4	11.8	0.460	0.410	14.0	335.0	133.7	133.7
H1-8199	1953	8	5.36	331.6	31.2	213.8	39.6	18.9	0.470	0.470	30.0	313.0	133.7	133.7
Average		8	8.29	338.0	30.1	216.9	36.1	33.2	0.752	0.465	53.0	293.6	136.1	136.1

Table 25 – Video data for ASX comparing with NAS.

Code	Month	Day	α	δ	λ–$\lambda_\odot$	β	V_g	e	q	i	ω	Ω	$\lambda_\odot$
SonotaCo	11	19.78	154.1	−6.4	281.4	−16.0	68.2	0.931	0.874	150.8	319.4	57.0	237.0
NAS			149.9	−3.4	281.7	−14.7							231.5

have recurrent nature, and KCG3 is the average year's activity (Paper II). Great Andromedid showers are remarkable but we can now record its trace by very patient study of video observations.

2. There are meteor showers being in sight or out of sight by limitations from characteristics of observing techniques.

Major showers are observable by every method: Quadrantids, Perseids, Geminids, and so on. Minor showers are difficult to detect by visual observations because they are low in HR. Many meteor showers have been reported by video observations recently but most of them might not be noticeable by other observations. On the other hand radar meteor showers might be not observable by other observations because of their characteristics. PPS locates near the apex, CTA is near the Taurid complex, and the discrimination of them from the background needs a huge volume of meteor data.

3. There are meteor showers only recognizable depending on the definition of a meteor shower.

There is no common definition for every meteor shower. Geobased and orbbased research have both merits and demerits. Meteor showers close to the ant-apex area are quite difficult objects for geobased research; TAH is a good example. It is necessary to keep in mind in the case of orbbased searches that the distance in D-criterion space is distorted by observational errors and by the characteristics of orbits; $D(M, N) < 0.15$ works well for discriminating KCG1, KCG2, and KCG3 but dissolves the trace of AND into pieces.

Acknowledgements

Figure 13 was kindly provided by Esko Lyytinen.

References

Brown P., Weryk R. J., Wong D. K., and Jones J. (2008). "A meteoroid stream survey using the Canadian Meteor Orbit Radar. I. Methodology and radiant catalogue". *Icarus*, **195**, 317–339.

Brown P., Wong D. K., Weryk R. J., and Wiegert P. (2010). "A meteoroid stream survey using the Canadian Meteor Orbit Radar. II. Identification of minor showers using a 3D wavelet transform". *Icarus*, **207**, 66–81.

Denning W. F. (1899). "General catalogue of the radiant points of meteoric showers and of fireballs and shooting stars observed at more than one station". *Mem. Roy. Astron. Soc.*, **53**, 203–292.

Hashimoto T. and Osada K. (1998). "June Bootid outburst: Optical observations from Japan". *WGN, Journal of the IMO*, **26:6**, 263–266.

Hawkins G. S., Southworth R. B., and Stienon F. (1959). "Recovery of the Andromedids". *Astron. J.*, **64**, 183–188.

IAUMDC (2013). `http://www.astro.amu.edu.pl/~jopek/MDC2007/` . (Updated 2013 Dec. 13, by Z. Kanuchova and T. J. Jopek).

Jenniskens P. (2006). *Meteor Showers and Their Parent Comets*. Cambridge University Press.

JPL (2014). "Small-body database browser". `http://ssd.jpl.nasa.gov/sbdb.cgi` .

Koseki M. (1978). "Reanalysis of Hoffmeister's observations". *19th Japanese Meteor Conference*. (In Japanese).

Koseki M. (1979). "Meteor radiant observed between 1928–69 in Japan". *The Heavens*, pages 60, 237, 270, 295. (In Japanese).

Koseki M. (1980). "Meteor radiant observed by the AMS". *21st Japanese Meteor Conference*. (In Japanese).

Koseki M. (1981). "Cluster analysis on meteor shower catalogues". *22nd Japanese Meteor Conference*. (In Japanese).

Koseki M. (1982). "Meteor shower research on photographic meteor database". *23rd Japanese Meteor Conference*. (In Japanese).

Koseki M. (1986). "Analysis of meteor data on a microcomputer system". *J. Brit. Astron. Assoc.*, **96**, 232–240.

Koseki M. (2009). "Meteor shower records: A reference table of observations from previous centuries". *WGN, Journal of the IMO*, **37:5**, 139–160.

Koseki M. (2012a). "A simple model of spatial structure of meteoroid streams". *WGN, Journal of the IMO*, **40:5**, 162–165.

Koseki M. (2012b). "Three components of 'Taurids'". *WGN, Journal of the IMO*, **40:4**, 129–138.

Koseki M. (2013). "How different view we see meteor showers by the different means: II and radar". *The 135th Meteor Science Seminar (MSS)*. (In Japanese).

Koseki M. (2014a). "Various meteor scenes I: The perception and the conception of a 'meteor shower'". *WGN, Journal of the IMO*, **42:5**, 170–180. (Paper I).

Koseki M. (2014b). "Various meteor scenes II: Cygnid-Draconid Complex (κ-Cygnids)". *WGN, Journal of the IMO*, **42:5**, 181–197. (Paper II).

Koseki M., Ueda M., and Shigeno Y. (2010). "What is the difference between image intensifier and CCD meteors? III. How do meteor showers look like by image intensifiers and by CCD?". *WGN, Journal of the IMO*, **38:5**, 145–160.

Lindblad B. A. (1971). "A computerized stream search among 2401 photographic meteor orbits". *Smithson. Contrib. Astrophys.*, **12**, 14–24.

Marsden B. G. (1989). *Catalogue of Cometary Orbits*. IAU Minor Planet Center, 6th edition.

Nakamura K. (1930). "On the observation of faint meteors, as experienced in the case of those from the orbit of comet Schwassmann-Wachmann, 1930d". *Mon. Not. Roy. Astron. Soc.*, **91**, 204–209.

Sato M. (2004). His prediction at `http://fas.kaicho.net/tenshow/meteor/7p2004/e1.htm` and the observational results of his group at `http://fas.kaicho.net/tenshow/meteor/pw2004/pw2004e.htm`.

Shigeno Y. and Yamamoto M.-Y. (2012). "Meteor shower catalog based on 3770 triangulation analyses of double-station image-intensified video observations over Japan". *WGN, Journal of the IMO*, **40:1**, 24–35.

Spaceweather (2010). "Minor meteor outburst". `http://www.spaceweather.com/archive.php?view=1&day=26&month=01&year=2010` .

Spaceweather (2013). "Meteor outburst in progress". `http://www.spaceweather.com/archive.php?view=1&day=08&month=12&year=2013` ; see also `view=1&day=09&month=12&year=2013` .

Terentjeva A. K. (1966). "A possible meteor streams' family of Pons-Winnecke periodic comet". *Problems of Cosmic Physics*, **1**, 40–46. (In Russian).

Handling Editor: David Asher

Preliminary results

Results of the IMO Video Meteor Network — September 2014

Sirko Molau[1], *Javor Kac*[2], *Stefano Crivello*[3], *Enrico Stomeo*[4], *Geert Barentsen*[5], *Rui Goncalves*[6], *Carlos Saraiva*[7], *Maciej Maciewski*[8], *and Mikhail Maslov*[9]

In 2014 September, more than 36 000 meteors were recorded by 81 cameras of the IMO Video Meteor Network cameras in more than 9 000 hours of observing time. Flux density profiles are presented for the α-Aurigids and September Perseids, based on meteors detected between 2011 and 2014. For the first time, it has been possible to use optical data from the Daytime Sextantids to present a flux density profile and to estimate the population index.

Received 2015 January 20

1 Introduction

A German proverb says "the first million is the hardest." We now have the evidence that this also holds true for meteor observation. Whereas it took us more than a decade from the start of the IMO Network in 1999 until November 2011 to record a million meteors, we needed less than 3 years for the second million. In September 2014 we reached that landmark – at the end of the month the counter was at 2 011 743 meteors. These had been recorded in 5 281 observing nights and 485 355 hours (or more than 50 years worth) of effective observing time.

September 2014 was comparable in productivity to the two preceding years. A total of 43 observers with 81 video cameras contributed to the IMO Network. The weather in September is often Indian summer like with nice observing conditions, and this year was no exception. 75 cameras were active on September 28, for example, and more than 2/3 of the cameras were able to collect data on twenty and more observing nights. The effective observing time of over 9 400 hours slightly surpassed the results of the last two years, the total of 36 000 meteors lies between those of 2012 and 2013 (Table 1 and Figure 1).

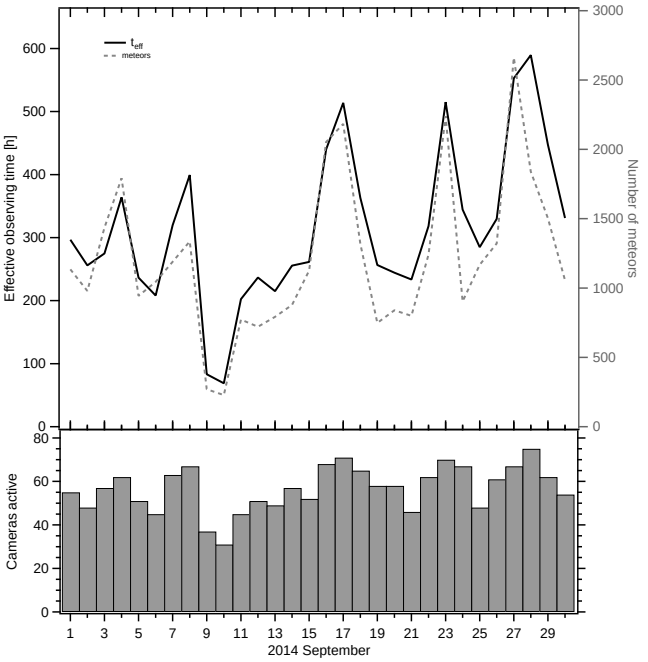

Figure 1 – Monthly summary for the effective observing time (solid black line), number of meteors (dashed gray line) and number of cameras active (bars) in 2014 September.

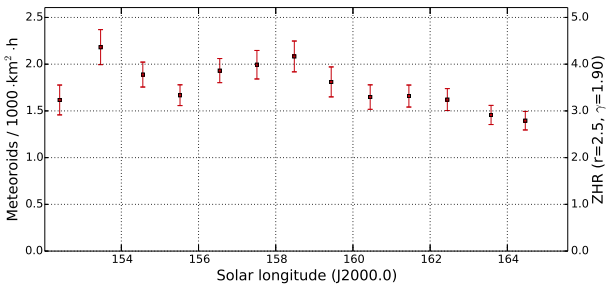

Figure 2 – Flux density profile of the α-Aurigids, averaged over IMO Video Meteor Network data of 2011–2014.

2 Perseus-Auriga showers

September offers a number of smaller meteor showers in the Perseus-Auriga region, but there are no major showers among them.

2.1 α-Aurigids

The α-Aurigids are active at the August/September boundary, but in neither 2014 nor the three preceding

[1]Abenstalstr. 13b, 84072 Seysdorf, Germany. Email: sirko@molau.de
[2]Na Ajdov hrib 24, 2310 Slovenska Bistrica, Slovenia. Email: javor.kac@orion-drustvo.si
[3]Via Bobbio 9a/18, 16137 Genova, Italy. Email: stefano.crivello@libero.it
[4]via Umbria 21/d, 30037 Scorze (VE), Italy. Email: stom@iol.it
[5]University of Hertfordshire, Hatfield AL10 9AB, United Kingdom. Email: geert@barentsen.be
[6]Urbanizacao da Boavista, Lote 46, Linhaceira, 2305-114 Asseiceira, Tomar, Portugal. Email: rui.goncalves@ipt.pt
[7]Rua Aquilino Ribeiro, 23 - 1 Dto. 2790028 Carnaxide, Portugal. Email: carlos.saraiva@netcabo.pt
[8]Wolynska 24, 22-100 Chelm, Poland. Email: mazziek@gmail.com
[9]16 Bronny, 90, Novosibirsk, Russia. Email: ast3@ngs.ru

IMO bibcode WGN-431-molau-vidsep
NASA-ADS bibcode 2015JIMO...43...28M

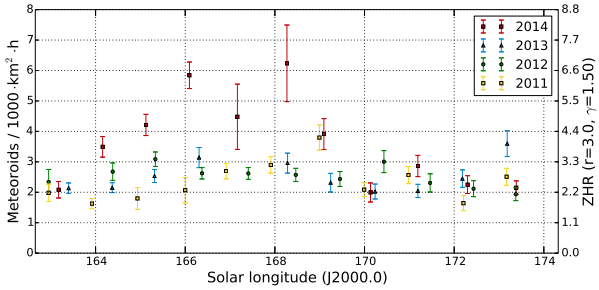

Figure 3 – Comparison of the flux density profiles of the September Perseids in 2011 to 2014. The outburst of 2013 September 9 is beyond the displayed range.

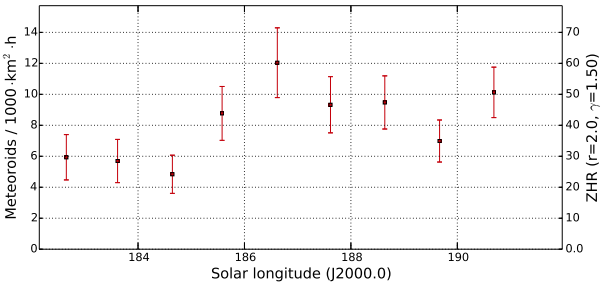

Figure 4 – Flux density profile of the Daytime Sextantids, averaged over IMO Video Meteor Network data of 2011–2014.

years did they show a well-defined activity profile. The flux density is fluctuating between 1.5 and 2 meteoroids per 1 000 km^2 per hour. With a little imagination, one may spot a weak maximum right at the change of month (Figure 2).

2.2 September Perseids

In "normal" years the September Perseids reach flux densities of between two and three meteoroids per 1 000 km^2 per hour, but this year we derived values almost twice as high (Figure 3). The graph does not show the 2013 outburst, which exceeds the selected y-axis range.

3 Daytime Sextantids

Jürgen Rendtel presented two daytime shower challenges at the last IMC (Rendtel, 2014). The Daytime Sextantids (DSX) in September are a second daytime shower (alongside the Daytime Arietids (ARI) of June) that can be observed rudimentarily in the optical domain thanks to their strength and the comparably large radiant distance from the Sun. Between 2011 and end of September 2014 we recorded an overall total of 200 Sextantids, twice as many as from the Daytime Arietids in June. The preliminary activity profile (not yet including the October 2014 data) shows a peak right at the September/October border with a flux density of more than 10 meteoroids per 1 000 km^2 per hour, although this value depends significantly on the selected zenith exponent (here: $\gamma = 1.5$). This activity would position the Daytime Sextantids somewhere between that of the Lyrids and Southern δ-Aquariids. As far as we know, this is the first activity profile based on optical observations.

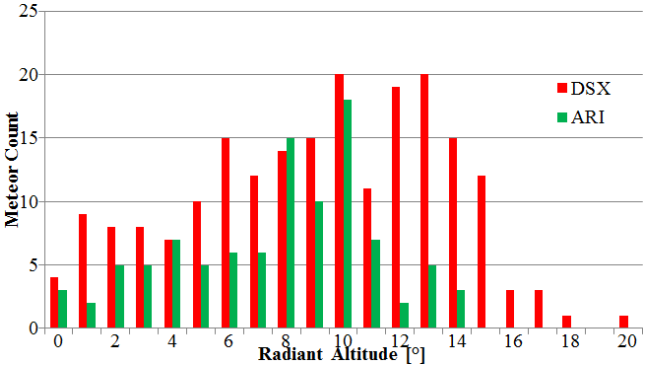

Figure 5 – Distribution of the observed Daytime Arietids and Daytime Sextantids against the radiant altitude.

Figure 5 compares the distribution of the observed Daytime Arietids and Sextantids against radiant altitude. In both cases, the radiant is about 35° away from the Sun. However, since the ecliptic is steeper in September than in June, the Daytime Sextantids can be observed slightly better. A few shower members were recorded at radiant altitudes beyond 15°.

If you have been assuming that daytime meteor showers are mainly observed at lower (brighter) limiting magnitudes at dawn, Figure 6 will correct this. It shows the cumulative distribution of Daytime Arietids and Sextantids as well as sporadic meteors (in the same observing nights) against the limiting magnitudes of the meteor cameras. Whereas there is indeed some deviation for the Daytime Arietids, the cumulative distribution of the Daytime Sextantids is almost identical to the distribution of the sporadic meteors.

The match between the curves hints of a similarity in population index for the Daytime Sextantids and sporadic meteors. Thus, we have been "brave" enough to calculate the population index for both showers. We combined all data from the activity periods in 2011 to 2014, and selected only three limiting magnitude intervals so as to maximize the available data set. The result looks quite promising (Figure 7): depending on the selected zenith exponent, the Daytime Arietids came out with a r-value around 2.2, and the Daytime Sextantids came out between 2.6 and 2.7. The population index of the sporadic meteors was determined to $r = 2.6$ during the Daytime Arietids and $r = 2.65$ during the Daytime Sextantids. That confirms that the Daytime Arietids have a noticeably smaller r-value than do sporadic meteors, those of the Daytime Sextantids and sporadics are virtually identical.

References

Rendtel J. (2014). "Daytime meteor showers". In Rault J.-L. and Roggemans P., editors, *Proceedings of the International Meteor Conference, Giron, France, 18–21 September, 2014*. International Meteor Organization, pages 93–97.

Handling Editor: Javor Kac

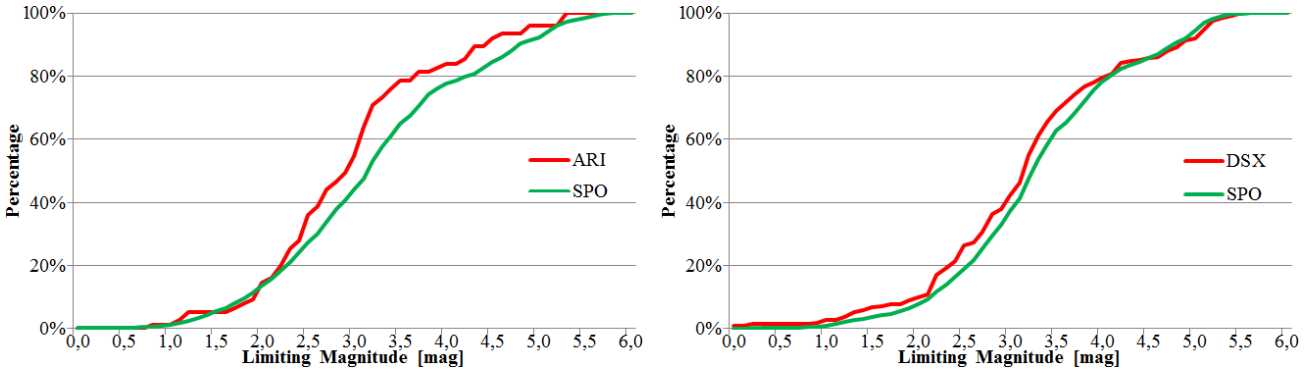

Figure 6 – Comparison of the cumulative distribution of the Daytime Arietids (left) and Daytime Sextantids (right) with sporadic meteors over the limiting magnitude of the camera.

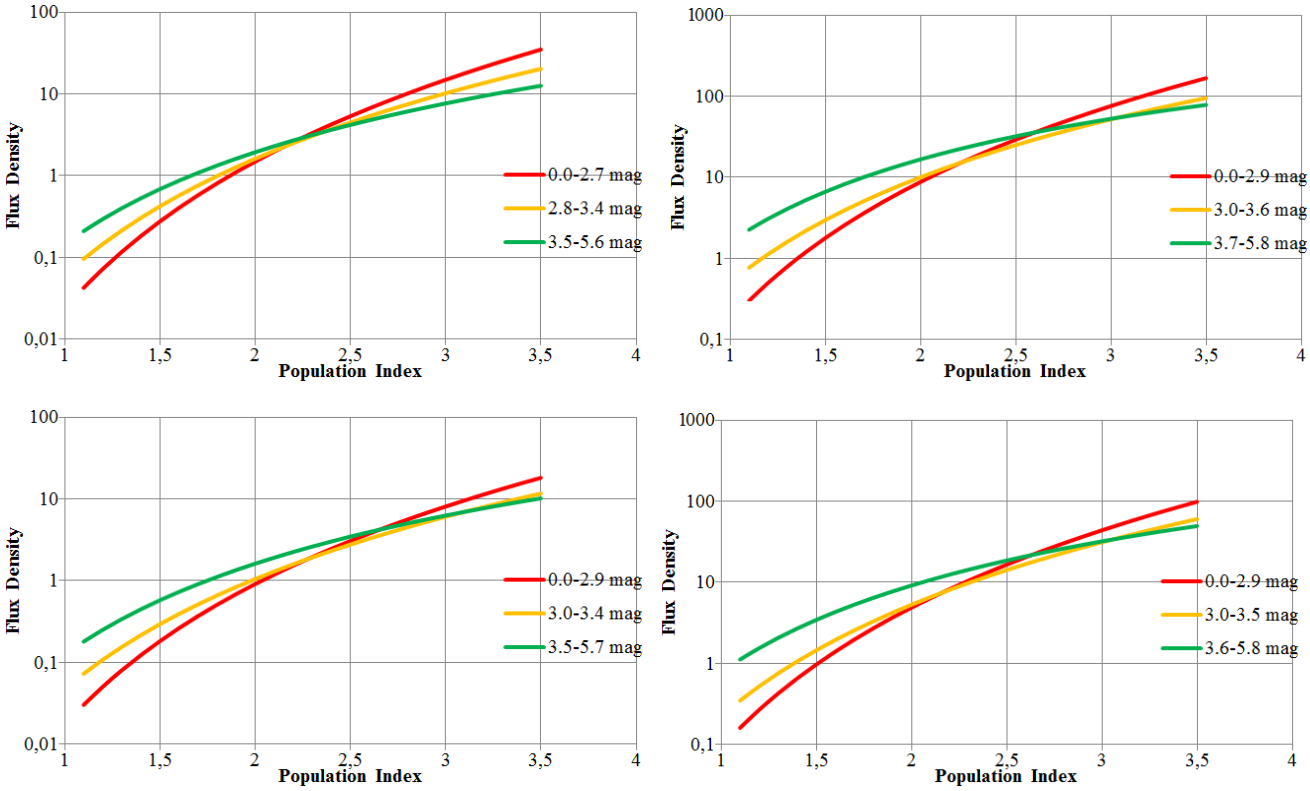

Figure 7 – Dependency of the flux density of the Daytime Arietids (upper left) and the Daytime Sextantids (upper right) as well as the sporadic meteors in the same time intervals (lower left and right) on the population index for different limiting magnitudes. The analysis is based on all observations of June 3–10 (left-hand figures) and September 24–October 10 (right-hand figures), respectively, in 2011–2014.

Code	Name	Location	Camera	FOV [°²]	Stellar LM [mag]	Eff.CA [km²]	Nights	Time [h]	Meteors
ARLRA	Arlt	Ludwigsfelde/DE	Ludwig2 (0.8/8)	1475	6.2	3779	23	129.3	944
BANPE	Bánfalvi	Zalaegerszeg/HU	Huvcse01 (0.95/5)	2423	3.4	361	9	17.7	93
BERER	Berkó	Ludányhalászi/HU	Hulud1 (0.8/3.8)	5542	4.8	3847	14	105.8	580
			Hulud3 (0.95/4)	4357	3.8	876	13	97.0	132
BOMMA	Bombardini	Faenza/IT	Mario (1.2/4.0)	5794	3.3	739	28	183.6	979
BREMA	Breukers	Hengelo/NL	Mbb3 (0.75/6)	2399	4.2	699	26	158.7	364
			Mbb4 (0.8/8)	1470	5.1	1208	23	144.7	282
BRIBE	Klemt	Herne/DE	Hermine (0.8/6)	2374	4.2	678	23	138.7	451
		Bergisch Gladbach/DE	Klemoi (0.8/6)	2286	4.6	1080	25	147.9	509
CASFL	Castellani	Monte Baldo/IT	Bmh1 (0.8/6)	2350	5.0	1611	27	148.5	534
			Bmh2 (1.5/4.5)*	4243	3.0	371	18	76.1	267
CRIST	Crivello	Valbrevenna/IT	Bilbo (0.8/3.8)	5458	4.2	1772	26	173.8	872
			C3P8 (0.8/3.8)	5455	4.2	1586	26	159.2	601
			Stg38 (0.8/3.8)	5614	4.4	2007	27	167.4	1095
CSISZ	Csizmadia	Baja/HU	Huvcse02 (0.95/5)	1606	3.8	390	15	24.6	104
DONJE	Donani	Faenza/IT	Jenni (1.2/4)	5886	3.9	1222	29	179.7	995
ELTMA	Eltri	Venezia/IT	Met38 (0.8/3.8)	5631	4.3	2151	20	105.2	394
FORKE	Förster	Carlsfeld/DE	Akm3 (0.75/6)	2375	5.1	2154	18	103.0	487
GONRU	Goncalves	Tomar/PT	Templar1 (0.8/6)	2179	5.3	1842	22	155.9	674
			Templar2 (0.8/6)	2080	5.0	1508	23	157.2	501
			Templar3 (0.8/8)	1438	4.3	571	26	160.0	273
			Templar4 (0.8/3.8)	4475	3.0	442	23	160.2	492
			Templar5 (0.75/6)	2312	5.0	2259	26	164.4	655
GOVMI	Govedič	Središče ob Dravi/SI	Orion2 (0.8/8)	1447	5.5	1841	10	46.1	223
			Orion3 (0.95/5)	2665	4.9	2069	17	80.2	134
			Orion4 (0.95/5)	2662	4.3	1043	14	74.5	135
HERCA	Hergenrother	Tucson/US	Salsa3 (1.2/4)*	2198	4.6	894	27	210.3	545
HINWO	Hinz	Schwarzenberg/DE	Hinwo1 (0.75/6)	2291	5.1	1819	16	97.7	456
IGAAN	Igaz	Baja/HU	Hubaj (0.8/3.8)	5552	2.8	403	19	102.8	182
		Hódmezővásárhely/HU	Huhod (0.8/3.8)	5502	3.4	764	21	107.8	200
		Budapest/HU	Hupol (1.2/4)	3790	3.3	475	14	74.6	43
JONKA	Jonas	Budapest/HU	Husor (0.95/4)	2286	3.9	445	16	94.3	175
KACJA	Kac	Ljubljana/SI	Orion1 (0.8/8)	1402	3.8	331	22	67.2	137
		Kamnik/SI	Cvetka (0.8/3.8)*	4914	4.3	1842	13	44.0	198
			Rezika (0.8/6)	2270	4.4	840	13	48.9	262
			Stefka (0.8/3.8)	5471	2.8	379	14	41.5	132
KISSZ	Kiss	Sülysáp/HU	Husul (0.95/5)*	4295	3.0	355	17	75.7	73
KOSDE	Koschny	Izana Obs./ES	Icc7 (0.85/25)*	714	5.9	1464	23	120.0	877
		La Palma/ES	Icc9 (0.85/25)*	683	6.7	2951	26	166.8	1754
		Noordwijkerhout/NL	Lic4 (1.4/50)*	2027	6.0	4509	22	143.7	450
LOJTO	Łojek	Grabniak/PL	Pav57 (1.0/5)	1631	3.5	269	12	74.2	102

Table 1 – Observers contributing to 2014 September data of the IMO Video Meteor Network. Eff.CA designates the effective collection area; the overall number of nights is the number of nights with at least one camera operating, the overall observing time and number of meteors are sums over all cameras.

Table 1 – Observers contributing to 2014 September data of the IMO Video Meteor Network – continued from previous page.

Code	Name	Location	Camera	FOV [°²]	Stellar LM [mag]	Eff.CA [km²]	Nights	Time [h]	Meteors
MACMA	Maciejewski	Chełm/PL	Pav35 (0.8/3.8)	5495	4.0	1584	27	183.7	530
			Pav36 (0.8/3.8)*	5668	4.0	1573	28	199.2	1065
			Pav43 (0.75/4.5)*	3132	3.1	319	27	169.2	427
			Pav60 (0.75/4.5)	2250	3.1	281	27	195.9	705
MARGR	Maravelias	Lofoupoli-Crete/GR	Loomecon (0.8/12)	738	6.3	2698	24	143.1	285
MARRU	Marques	Lisbon/PT	Ran1 (1.4/4.5)	4405	4.0	1241	20	138.2	336
MASMI	Maslov	Novosibirsk/RU	Nowatec (0.8/3.8)	5574	3.6	773	18	85.4	622
MOLSI	Molau	Seysdorf/DE	Avis2 (1.4/50)*	1230	6.9	6152	24	144.0	1280
			Mincam1 (0.8/8)	1477	4.9	1084	23	120.8	693
		Ketzür/DE	Remo1 (0.8/8)	1467	6.5	5491	26	140.6	1081
			Remo2 (0.8/8)	1478	6.4	4778	25	138.5	726
			Remo3 (0.8/8)	1420	5.6	1967	24	127.8	519
			Remo4 (0.8/8)	1478	6.5	5358	24	147.0	924
MOSFA	Moschner	Rovereto/IT	Rover (1.4/4.5)	3896	4.2	1292	25	36.9	235
OCHPA	Ochner	Albiano/IT	Albiano (1.2/4.5)	2944	3.5	358	19	102.3	324
OTTMI	Otte	Pearl City/US	Orie1 (1.4/5.7)	3837	3.8	460	26	155.7	305
PERZS	Perkó	Becsehely/HU	Hubec (0.8/3.8)*	5498	2.9	460	20	109.5	525
PUCRC	Pucer	Nova vas nad Dragonjo/SI	Mobcam1 (0.75/6)	2398	5.3	2976	20	99.3	371
ROTEC	Rothenberg	Berlin/DE	Armefa (0.8/6)	2366	4.5	911	19	112.0	278
SARAN	Saraiva	Carnaxide/PT	Ro1 (0.75/6)	2362	3.7	381	21	142.8	218
			Ro2 (0.75/6)	2381	3.8	459	24	136.7	312
			Ro3 (0.8/12)	710	5.2	619	24	155.4	503
			Sofia (0.8/12)	738	5.3	907	23	147.8	249
SCALE	Scarpa	Alberoni/IT	Leo (1.2/4.5)*	4152	4.5	2052	20	86.3	276
SCHHA	Schremmer	Niederkrüchten/DE	Doraemon (0.8/3.8)	4900	3.0	409	28	120.3	420
SLAST	Slavec	Ljubljana/SI	Kayak1 (1.8/28)	563	6.2	1294	1	0.5	3
STOEN	Stomeo	Scorze/IT	Min38 (0.8/3.8)	5566	4.8	3270	27	122.1	763
			Noa38 (0.8/3.8)	5609	4.2	1911	26	131.5	596
			Sco38 (0.8/3.8)	5598	4.8	3306	26	131.1	810
STRJO	Strunk	Herford/DE	Mincam2 (0.8/6)	2354	5.4	2751	25	134.0	338
			Mincam3 (0.8/6)	2338	5.5	3590	25	120.6	407
			Mincam4 (1.0/2.6)	9791	2.7	552	25	115.5	279
			Mincam5 (0.8/6)	2349	5.0	1896	24	119.2	326
			Mincam6 (0.8/6)	2395	5.1	2178	24	120.0	305
TEPIS	Tepliczky	Agostyán/HU	Huago (0.75/4.5)	2427	4.4	1036	20	83.2	183
			Humob (0.8/6)	2388	4.8	1607	21	91.7	313
TRIMI	Triglav	Velenje/SI	Sraka (0.8/6)*	2222	4.0	546	16	37.3	92
YRJIL	Yrjölä	Kuusankoski/FI	Finexcam (0.8/6)	2337	5.5	3574	24	143.9	482
ZELZO	Zelko	Budapest/HU	Huvcse03 (1.0/4.5)	2224	4.4	933	3	14.6	31
			Huvcse04 (1.0/4.5)	1484	4.4	573	3	9.8	25
* active field of view smaller than video frame						Overall	30	9 448.3	36 518

Results of the IMO Video Meteor Network — October 2014

Sirko Molau[1], *Javor Kac*[2], *Stefano Crivello*[3], *Enrico Stomeo*[4], *Geert Barentsen*[5], *Rui Goncalves*[6], *Carlos Saraiva*[7], *Maciej Maciewski*[8], *and Mikhail Maslov*[9]

A record number of 86 cameras of the IMO Video Meteor Network collected over 11 000 hours worth of data in 2014 October, recording almost 52 000 meteors. Yearly flux density profiles are presented for the Orionids, Leonis Minorids, October Camelopardalids, and October Ursae Majorids, covering the period from 2011 to 2014. Population indexes are calculated for all four meteor showers.

Received 2015 February 25

1 Introduction

October regaled observers with unusually good weather conditions, even though there were regional differences. The observing conditions in Poland and Germany were close to perfect. More southerly located observers, however, had to cope with a few cloudy nights in the first third of the month. In addition, the Orionids were clouded out from some locations.

The number of meteor cameras increased to the all-time high of 86, with up to 71 being active in parallel (October 19/20). Our new observer Rui Marquez put the second camera CAB1 in operation. In addition the camera ESCIMO of Sirko Molau, which had been inactive for many years, was resurrected as will be described later in detail.

Fifty seven cameras collected data on twenty or more nights (Table 1 and Figure 1). The cumulative effective observing time was 11 200 hours, which is more than we have collected in any previous October, and, after March 2014, the second best ever total. In that time, almost 52 000 meteors were recorded, which is again more than in previous years. Only in 2011, when there was exceptional Orionid activity, did we record more meteors in October.

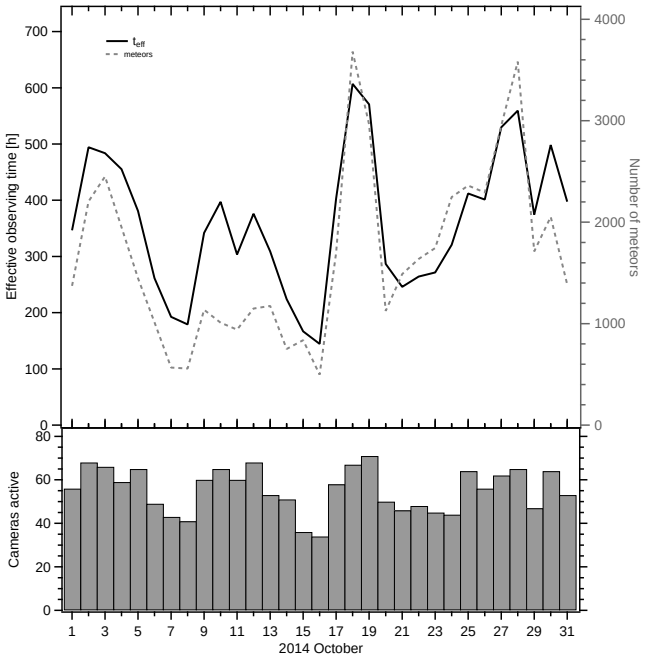

Figure 1 – Monthly summary for the effective observing time (solid black line), number of meteors (dashed gray line) and number of cameras active (bars) in 2014 October.

2 Orionids

The most important meteor shower of October are the Orionids. The Orionid (8 ORI) peak of 2014 coincided well with the new Moon, which promised good observing conditions. However, the years of enhanced activity are over for now, so that only "normal" zenithal hourly rates below 20 were expected and this was confirmed by the quick-look-analysis of IMO (International Meteor Organization, 2014). Only in a single interval did the ZHR exceed 20, otherwise it remained in the 10 to 15 range. This contrasts with 2012, when a peak ZHR of 25 was still being reported (International Meteor Organization, 2013).

Exactly the same picture is seen in the video data of the IMO Network (Figure 2). In 2011, we measured flux densities of up to 25 meteoroids per 1 000 km^2 per hour

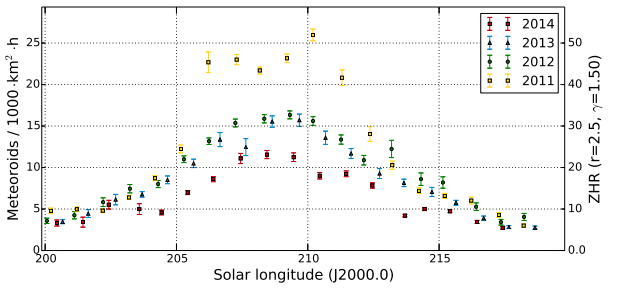

Figure 2 – Flux density profile of the Orionids 2011–2014, derived from observations of the IMO Video Meteor Network.

[1]Abenstalstr. 13b, 84072 Seysdorf, Germany. Email: sirko@molau.de
[2]Na Ajdov hrib 24, 2310 Slovenska Bistrica, Slovenia. Email: javor.kac@orion-drustvo.si
[3]Via Bobbio 9a/18, 16137 Genova, Italy. Email: stefano.crivello@libero.it
[4]via Umbria 21/d, 30037 Scorze (VE), Italy. Email: stom@iol.it
[5]University of Hertfordshire, Hatfield AL10 9AB, United Kingdom. Email: geert@barentsen.be
[6]Urbanizacao da Boavista, Lote 46, Linhaceira, 2305-114 Asseiceira, Tomar, Portugal. Email: rui.goncalves@ipt.pt
[7]Rua Aquilino Ribeiro, 23 - 1 Dto. 2790028 Carnaxide, Portugal. Email: carlos.saraiva@netcabo.pt
[8]Wolynska 24, 22-100 Chelm, Poland. Email: mazziek@gmail.com
[9]16 Bronny, 90, Novosibirsk, Russia. Email: ast3@ngs.ru

IMO bibcode WGN-431-molau-vidoct
NASA-ADS bibcode 2015JIMO...43...33M

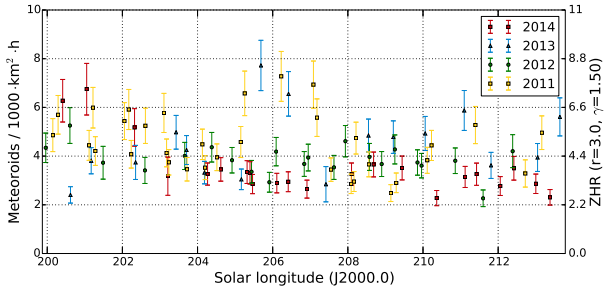

Figure 3 – Flux density profile of the ε-Geminids 2011–2014, derived from observations of the IMO Video Meteor Network.

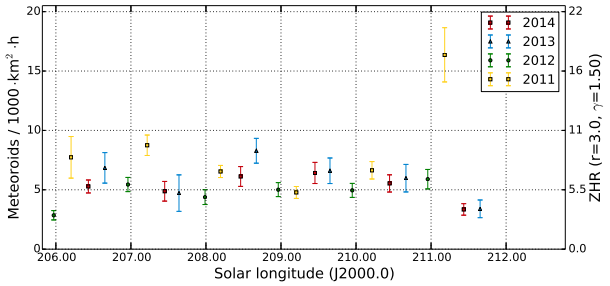

Figure 4 – Flux density profile of the Leonis Minorids 2011–2014, derived from observations of the IMO Video Meteor Network.

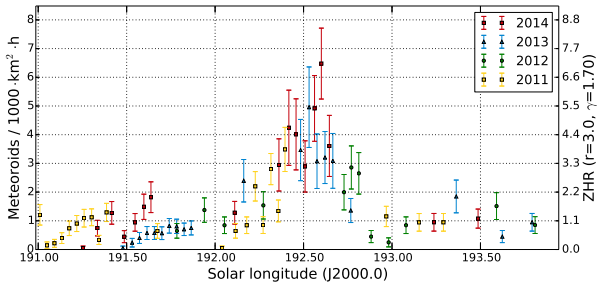

Figure 5 – Flux density profile of the October Camelopardalids 2011–2014, derived from observations of the IMO Video Meteor Network.

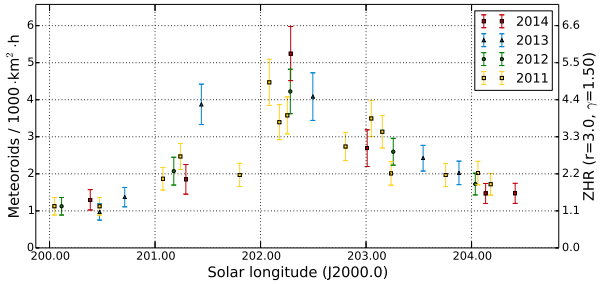

Figure 6 – Flux density profile of the October Ursae Majorids 2011–2014, derived from observations of the IMO Video Meteor Network.

(Molau et al., 2012). This figure reduced to values near 15 in 2012 and 2013 (Molau et al., 2013; Molau et al., 2014b), and in 2014 they declined again by 20%. Hence in 2014 we measured roughly half of the flux density of 2011, confirming that the Orionids are back at the standard activity level.

2.1 ε-Geminids

At about the same time the ε-Geminids (23 EGE) are active. We do not obtain a clear activity profile for this shower. 2011 and 2013 left the impression that there might be a peak between 205° and 207° solar longitude. However, the data of 2012 and 2014 do not show this peak (Figure 3).

2.2 Leonis Minorids

The activity profile of the Leonis Minorids (22 LMI) is flat as well, if we ignore a single outlier on 2011 October 24/25 (Figure 4). The flux density reaches typically values of about 6 meteoroids per 1 000 km^2 per hour, which is slightly more than what we see from the ε-Geminids.

3 October Camelopardalids

The October Camelopardalids (281 OCT) are renowned for their short peak (FWHM 6 hours) centered at 192°.6 solar longitude. This year the peak fell into the European morning hours of October 6, so chances were good to detect the shower again. That is what indeed happened – at exactly the expected time we found a clear increase in rates (Figure 5). The flux density reaches values of more than 5 meteoroids per 1 000 km^2 per hour. This time we had to choose a zenith exponent of $\gamma = 1.7$ to smooth the activity profile.

4 October Ursae Majorids

The October Ursae Majorids (333 OCU) are a shower that was discovered in the late 2000s with a maximum a few days before the Orionids. The shower can be detected every year in our video data thanks to its high declination and a flux density of 5 meteoroids per 1 000 km^2 per hour at maximum.

5 Population indexes

Afterwards we calculated the population index for all showers (Figure 7). The r-value of the sporadic meteors varied around 2.5 in the first half of the month with single upward outliers. Just at the Orionid peak, however, we find a clear minimum with r-values down to 2.0.

The population index of the October Camelopardalids is 2.1 on October 5/6, i.e. about 0.5 smaller than the value for sporadic meteors. For the October Ursae Majorids we also derive a r-value of 2.1. In this case, we combined the data of all relevant nights in order to have sufficient statistics. Once again the r-value is smaller than for the sporadic meteors.

In case of the ε-Geminids, we combined the data of four consecutive nights. Their population index is comparable to that of the sporadic meteors.

The Orionids show a well-defined population index profile. It starts at $r = 2.6$ and decreases to a value

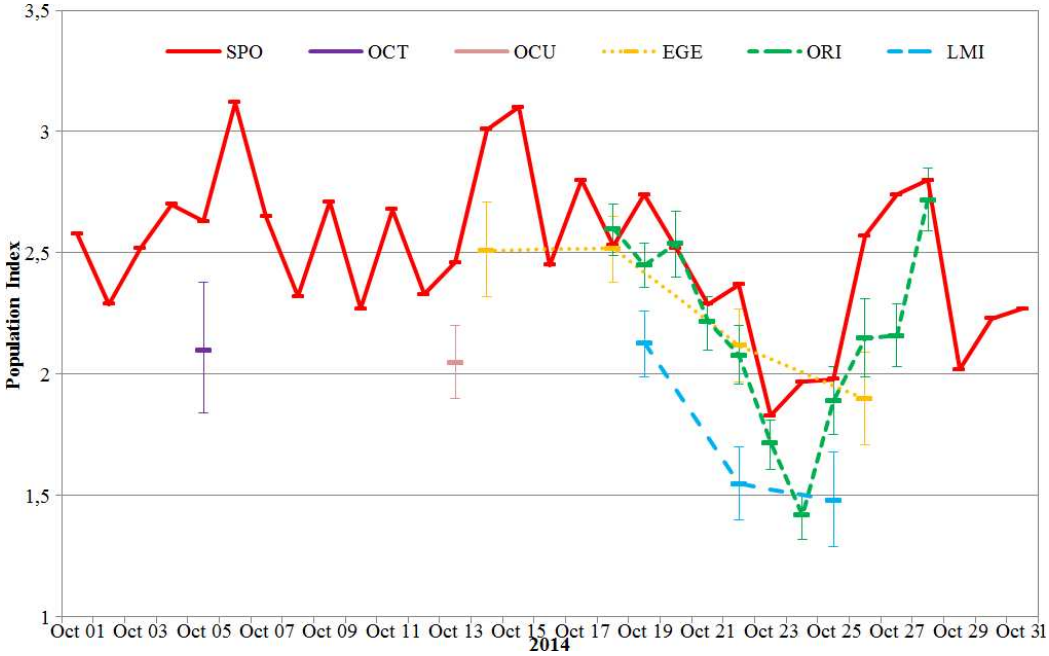

Figure 7 – Population index for different meteor showers and sporadic meteors in October 2014.

of 1.4 on October 24. Thereafter it rises again to 2.7. Even though the time of the minimum coincides with the sporadic minimum, we can still conclude that the Orionids also have a larger fraction of bright meteors than do the sporadics.

Last but not least we averaged the Leonis Minorid observations over three consecutive nights. Their population index values are more than 0.5 below the sporadic value, which means that this shower has a particularly high percentage of bright meteors.

Note that the intersection point of graphs in the flux density vs. population index plot is much more precise for minor showers (OCT, OCU, EGE, LMI) with roughly 200 meteors per data point. In case of ORI and SPO with more meteors, there is often no well-defined intersection point.

The population index analysis was continued in a different fashion in October. At the 2014 IMC, Molau (2014) had presented a new procedure to derive r-values from heterogeneous video data. Discussion with other IMC participants underlined that the procedure would be more precise the larger the covered limiting magnitude range. We typically use Mintron cameras (e.g. MINCAM1) with 8 mm $f/0.8$ Computar lens, which yields a field of view of 43° × 32° (1 474 square degrees). Depending on the sky quality, such cameras obtain stellar limiting magnitudes between 6.0 and 6.5 mag. The image-intensified camera AVIS2 goes down even fainter to 7.0 mag within the 1 230 square degrees field of view. So after the IMC Sirko Molau started to experiment with lenses of longer focal length to check whether this will increase the limiting magnitude range in a sensible way. At first he equipped a Mintron camera with a 1" $f/0.85$ c-mount lens from Fujinon with 25 mm focal length. In this setup, the field of view is reduced to 14° × 11° (155 square de-

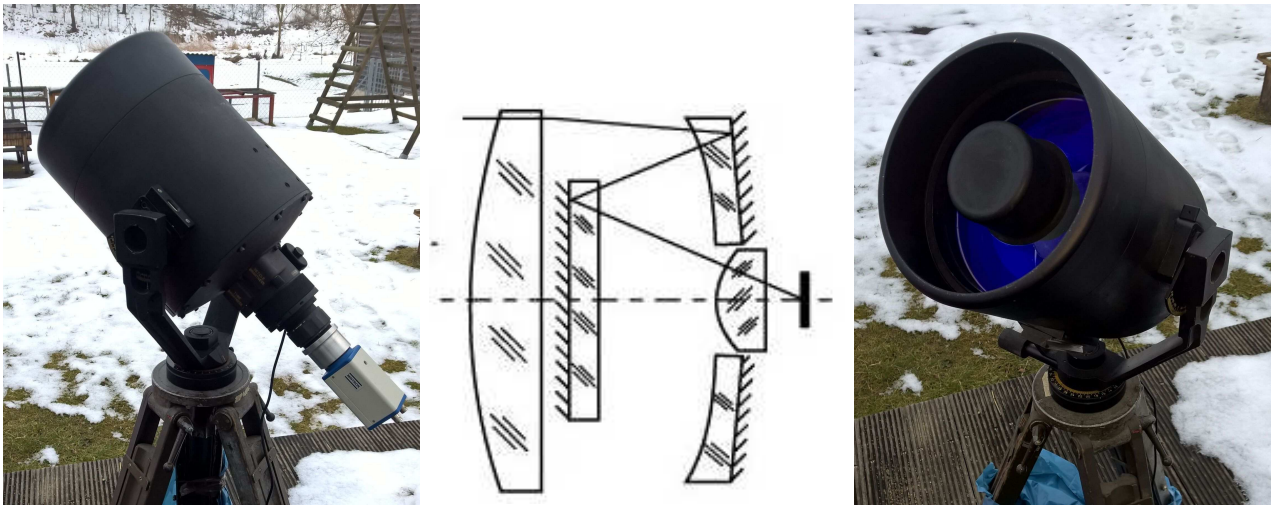

Figure 8 – The image-intensified camera ESCIMO and a schematic drawing of an aplanatic mirror system after Flügge (from `http://www.spektrum.de/lexikon/optik/aplanatische-spiegelsysteme/189`).

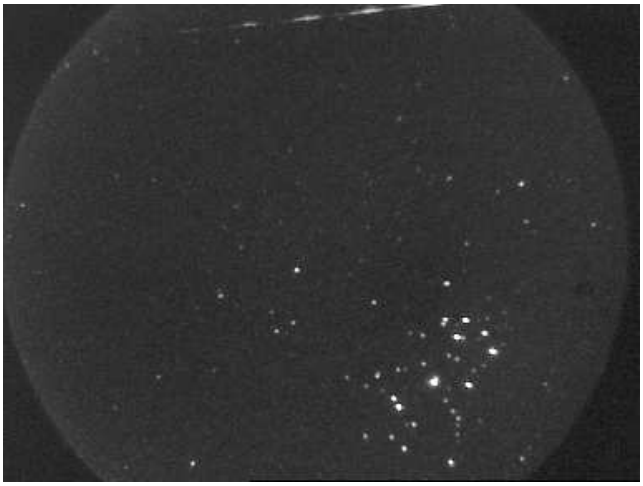

Figure 9 – A 13°/s Geminid near the Pleiades, recorded by Escimo on 2014 December 12.

grees), but the camera reaches a limiting magnitude of 7.7 mag. Thereafter a special camera Escimo was tested. This contains an aplanatic mirror system after Flügge (similar to a Schmidt-Cassegrain telescope with a large secondary mirror) with integrated 25 mm Gen II image intensifier. The circular field of view of this camera with military origin has a diameter of 5.°5, corresponding to a field of view of 22 square degrees and it reaches a stellar limiting magnitude of 10.0 mag (Figure 8). If this image-intensified camera is compared to a 1/2" Mintron camera, you derive an effective focal length of 65 mm with a free aperture of 220 mm. In order to be able to process observations with Escimo, MetRec had to be extended first. Based on the Tycho-2 catalog, the software can now detect stars up to 11 mag, whereas the limit was 8 mag before.

Hence the gain in stellar limiting magnitude achieved via these setups is 1.7 and 4.0 mag, respectively. Depending on the population index r, this translates into a gain in meteor counts by the factor of $r^{1.7}$ and $r^{4.0}$, respectively. Would that be sufficient to compensate for the loss in field of view by a factor of 9.5 and 67, respectively?

Practical tests between 2014 October and 2015 January showed that both cameras are better at recording slower meteors (Figure 9). That is no surprise, since a meteor with 30°/s angular velocity needs at most 5 video frames to cross the complete field of view. The gap between stellar and meteor limiting magnitude is particularly large for such small fields of view. So in total the cameras record fewer meteors than does the reference camera Mincam1.

For a more detailed analysis, we compared the meteor limiting magnitude and the effective collection area of all the setups. The calculation was based on the night of October 20/21 with identical alignment of all cameras. They were pointing towards southeast at medium altitude above the horizon.

Let us start with a slow meteor shower, the Northern Taurids. At the begin of night, the radiant is less than 20° away from the field of view, and the meteors are moving on average with 2°/s in the field of view. By the end of the night, the radiant distance has increased to 90° and the angular velocity has increased to 12°/s (Figure 10, upper left).

At the start of night, the meteor limiting magnitude varied between 5.2 (Mincam1) and 8.1 mag (Escimo). Towards the end of the night they were decreasing to values between 4.5 and 6.1 mag due to the increasing angular velocity (Figure 11, left). Hence, the loss in limiting magnitude due to the motion of meteors amounts to 0.8 and 1.9 mag, respectively at first, and then to values between 1.5 mag (Mincam1) and almost 4 mag (Escimo). In addition, there is a lower detection limit in MetRec of 1.5°/s meteor velocity to avoid the false detection of satellites. Thus, Escimo is partly blind for Taurids at the start of night. It is no surprise that the effective collection areas (calculated with $r = 2.3$) of the more powerful cameras falls well behind the reference system (Figure 11, right). The camera with 25 mm lens has only 19% of the Taurid collection area in the course of the night, and it is only 8% for Escimo.

At the start of night, the Orionid radiant is 60° away from the field of view and shower meteors are moving at roughly 20°/s. After midnight the radiant reaches the smallest distance of about 15°, and the apparent meteor velocity drops to 6°/s, before the values are increasing again towards the morning hours (Figure 10, right). At the start of night, the Orionid limiting magnitude varies between 3.9 and 5.6 mag, which corresponds to a loss between 2.1 (Mincam1) and 4.4 magnitudes (Escimo). After midnight the meteor limiting magnitude reaches values between 5.1 and 8.1 mag, i.e. the loss reduces to between 0.9 and 1.9 mag thanks to the smaller radiant distance (Figure 12, left). For this faster shower, the reduction in effective collection area (calculated with $r = 2.5$) is nearly the same – it reduces to 20% and 10%, respectively, of the value from the reference camera Mincam1 (Figure 12, right).

The radiant distance of the Leonis Minorids decreases from over 100° in the evening (when the radiant is just rising) to 30° at dawn. In parallel, the apparent meteor velocity reduces from an average value of 22°/s down to 11°/s. The meteor limiting magnitude varies between 3.9 and 5.6 mag, which is equivalent to a loss in limiting magnitude between 2.1 magnitudes for Mincam1 and 4.4 for Escimo. At dawn, the limiting meteor magnitude varies between 4.5 and 6.2 mag, i.e. the loss reduces to values between 1.5 and 3.8 mag (Figure 13, left). Given a population index of 3.0, the effective collection area reduces to 15% and 8%, respectively, relative to the reference camera Mincam1 (Figure 13, right).

Bottom line: Cameras with longer focal lengths can indeed increase the limiting magnitude range by 2 to 3 mag, whereby the gain is biggest for slow meteor showers. However, this gain in limiting magnitude comes at the cost of a significantly reduction of the field of view, so that the effective collection area and the number of recorded meteors reduce by about one order of magnitude. The use of lenses with very long focal length is only worthwhile in case of major showers with good observed rates.

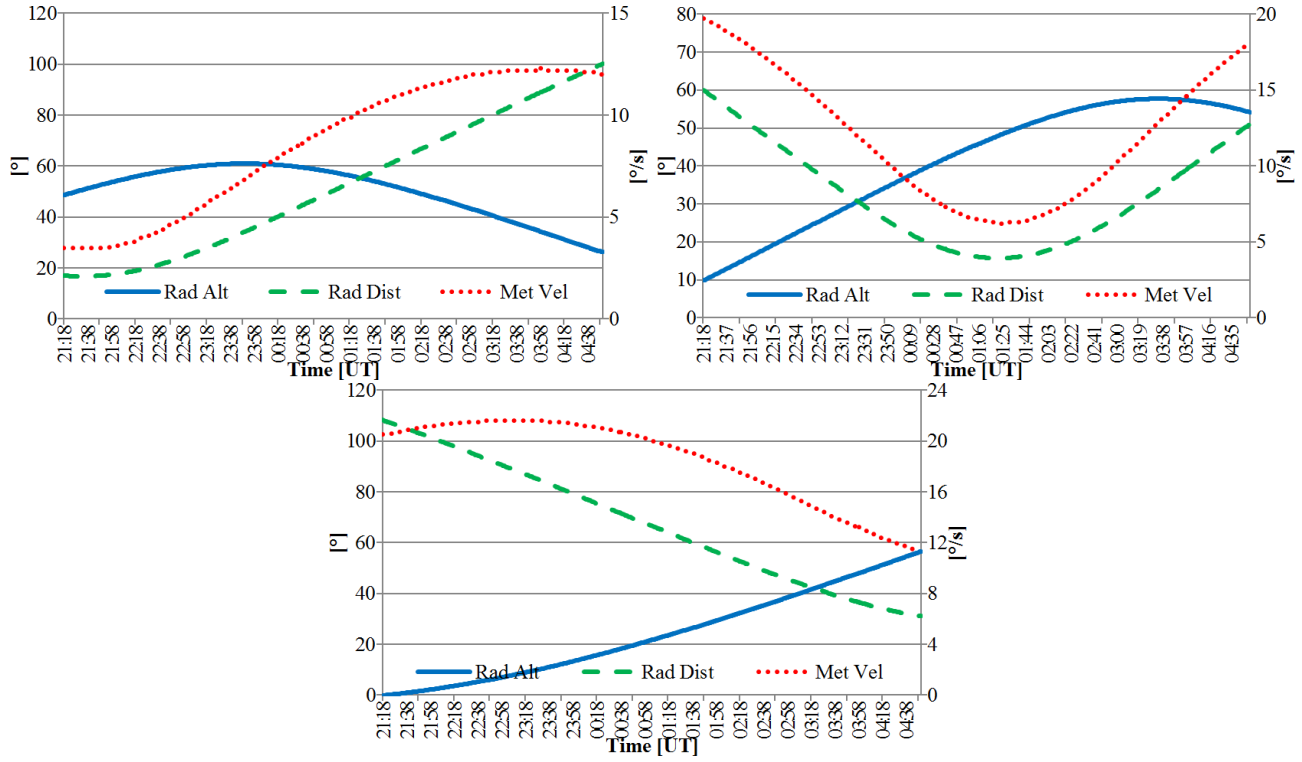

Figure 10 – Boundary conditions for the comparison of different cameras pointing towards southeast at medium altitude on October 20/21: Radiant altitude (Rad Alt) in °, mean radiant distance from the field of view (Rad Dist) in ° and mean apparent meteor velocity (Met Vel) in °/s. The values are shown for the northern Taurids (upper left), Orionids (upper right), and Leonis Minorids (lower).

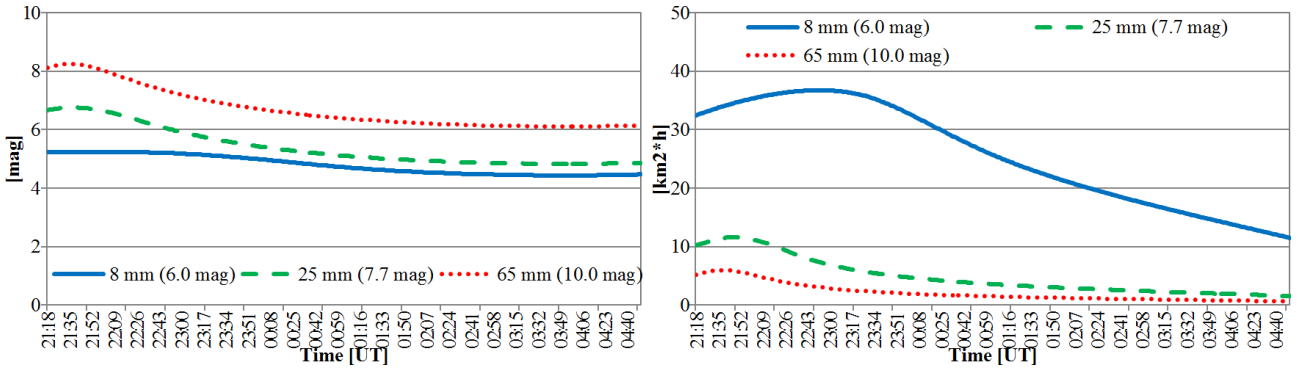

Figure 11 – Meteor limiting magnitude (left) and effective collection area (right) for the Northern Taurids, calculated for three cameras with different focal lengths and stellar limiting magnitudes between 6.0 and 10.0 mag.

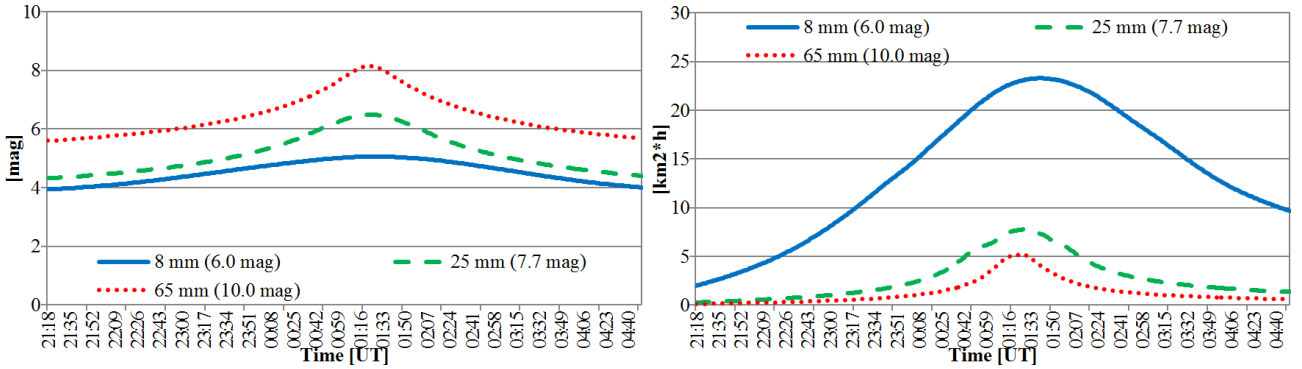

Figure 12 – Meteor limiting magnitude (left) and effective collection area (right) for the Orionids, calculated for three cameras with different focal lengths and stellar limiting magnitudes between 6.0 and 10.0 mag.

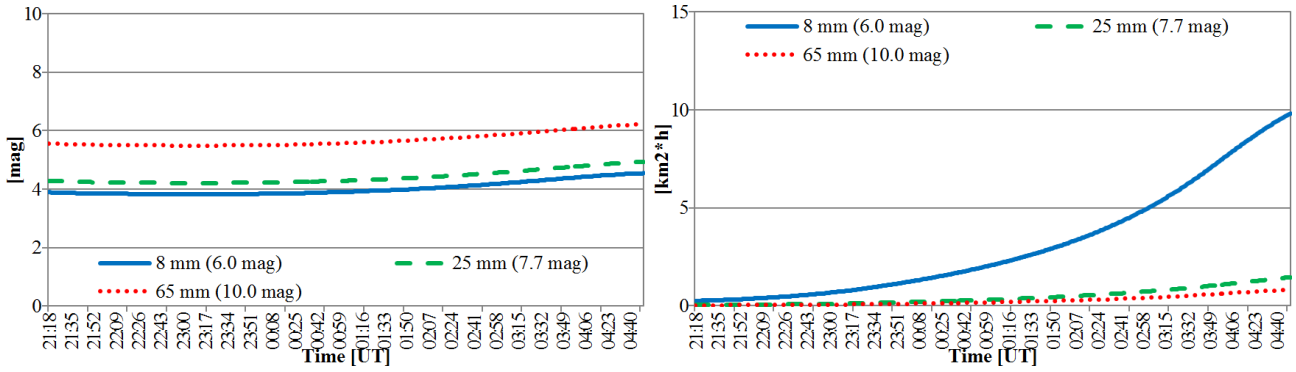

Figure 13 – Meteor limiting magnitude (left) and effective collection area (right) for the Leonis Minorids, calculated for three cameras with different focal lengths and stellar limiting magnitudes between 6.0 and 10.0 mag.

References

International Meteor Organization (2013). "Orionids 2012: visual data quicklook". `http://www.imo.net/live/orionids2012` .

International Meteor Organization (2014). "Orionids 2014: visual data quicklook". `http://www.imo.net/live/orionids2014` .

Molau S., Barentsen G., and Crivello S. (2014a). "Obtaining population indices from video observations of meteors". In Rault J.-L. and Roggemans P., editors, *Proceedings of the International Meteor Conference, Giron, France, 18–21 September, 2014*. International Meteor Organization, pages 74–80.

Molau S., Kac J., Berko E., Crivello S., Stomeo E., Igaz A., and Barentsen G. (2012). "Results of the IMO Video Meteor Network – October 2011". *WGN, Journal of the IMO*, **40:1**, 41–47.

Molau S., Kac J., Berko E., Crivello S., Stomeo E., Igaz A., Barentsen G., and Goncalves R. (2013). "Results of the IMO Video Meteor Network – October 2012". *WGN, Journal of the IMO*, **41:1**, 23–30.

Molau S., Kac J., Crivello S., Stomeo E., Barentsen G., and Goncalves R. (2014b). "Results of the IMO Video Meteor Network – October 2013". *WGN, Journal of the IMO*, **42:1**, 20–24.

Handling Editor: Javor Kac

Code	Name	Location	Camera	FOV [°²]	Stellar LM [mag]	Eff.CA [km²]	Nights	Time [h]	Meteors
ARLRA	Arlt	Ludwigsfelde/DE	Ludwig2 (0.8/8)	1475	6.2	3779	25	130.9	1190
BANPE	Bánfalvi	Zalaegerszeg/HU	Huvcse01 (0.95/5)	2423	3.4	361	15	46.4	246
BERER	Berkó	Ludányhalászi/HU	Hulud1 (0.8/3.8)	5542	4.8	3847	18	142.4	730
			Hulud3 (0.95/4)	4357	3.8	876	17	130.9	212
BOMMA	Bombardini	Faenza/IT	Mario (1.2/4.0)	5794	3.3	739	30	205.9	1107
BREMA	Breukers	Hengelo/NL	Mbb3 (0.75/6)	2399	4.2	699	20	126.9	355
			Mbb4 (0.8/8)	1470	5.1	1208	20	115.5	272
BRIBE	Klemt	Herne/DE	Hermine (0.8/6)	2374	4.2	678	24	134.4	528
		Bergisch Gladbach/DE	Klemoi (0.8/6)	2286	4.6	1080	23	125.7	521
CASFL	Castellani	Monte Baldo/IT	Bmh1 (0.8/6)	2350	5.0	1611	19	153.9	816
			Bmh2 (1.5/4.5)*	4243	3.0	371	13	128.2	615
CRIST	Crivello	Valbrevenna/IT	Bilbo (0.8/3.8)	5458	4.2	1772	24	183.8	1259
			C3P8 (0.8/3.8)	5455	4.2	1586	22	183.4	917
			Stg38 (0.8/3.8)	5614	4.4	2007	23	175.6	1477
CSISZ	Csizmadia	Baja/HU	Huvcse02 (0.95/5)	1606	3.8	390	22	96.9	266
DONJE	Donani	Faenza/IT	Jenni (1.2/4)	5886	3.9	1222	30	211.2	1327
ELTMA	Eltri	Venezia/IT	Met38 (0.8/3.8)	5631	4.3	2151	25	171.7	830
FORKE	Förster	Carlsfeld/DE	Akm3 (0.75/6)	2375	5.1	2154	21	150.1	794
GONRU	Goncalves	Tomar/PT	Templar1 (0.8/6)	2179	5.3	1842	22	192.3	1087
			Templar2 (0.8/6)	2080	5.0	1508	23	198.6	837
			Templar3 (0.8/8)	1438	4.3	571	22	191.3	421
			Templar4 (0.8/3.8)	4475	3.0	442	23	200.5	893
			Templar5 (0.75/6)	2312	5.0	2259	24	197.4	848
GOVMI	Govedič	Središče ob Dravi/SI	Orion2 (0.8/8)	1447	5.5	1841	20	112.0	584
			Orion3 (0.95/5)	2665	4.9	2069	20	109.0	246
			Orion4 (0.95/5)	2662	4.3	1043	11	71.7	142
HERCA	Hergenrother	Tucson/US	Salsa3 (1.2/4)*	2198	4.6	894	26	261.8	845
HINWO	Hinz	Schwarzenberg/DE	Hinwo1 (0.75/6)	2291	5.1	1819	24	188.2	1119
IGAAN	Igaz	Baja/HU	Hubaj (0.8/3.8)	5552	2.8	403	23	130.2	282
		Hódmezővásárhely/HU	Huhod (0.8/3.8)	5502	3.4	764	23	134.0	382
		Budapest/HU	Hupol (1.2/4)	3790	3.3	475	12	28.6	60
JONKA	Jonas	Budapest/HU	Husor (0.95/4)	2286	3.9	445	18	146.1	294
KACJA	Kac	Ljubljana/SI	Orion1 (0.8/8)	1402	3.8	331	23	87.4	150
		Kamnik/SI	Cvetka (0.8/3.8)*	4914	4.3	1842	18	86.1	406
			Rezika (0.8/6)	2270	4.4	840	20	95.8	574
			Stefka (0.8/3.8)	5471	2.8	379	14	79.1	268
		Kostanjevec/SI	Metka (0.8/12)*	715	6.4	640	5	35.9	191
KISSZ	Kiss	Sülysáp/HU	Husul (0.95/5)*	4295	3.0	355	20	120.3	107
KOSDE	Koschny	Izana Obs./ES	Icc7 (0.85/25)*	714	5.9	1464	17	139.1	1233
		La Palma/ES	Icc9 (0.85/25)*	683	6.7	2951	22	131.8	1330
		Noordwijkerhout/NL	Lic4 (1.4/50)*	2027	6.0	4509	18	97.7	321
LOJTO	Łojek	Grabniak/PL	Pav57 (1.0/5)	1631	3.5	269	19	133.0	318

Table 1 – Observers contributing to 2014 October data of the IMO Video Meteor Network. Eff.CA designates the effective collection area; the overall number of nights is the number of nights with at least one camera operating, the overall observing time and number of meteors are sums over all cameras.

Table 1 – Observers contributing to 2014 October data of the IMO Video Meteor Network – continued from previous page.

Code	Name	Location	Camera	FOV [°²]	Stellar LM [mag]	Eff.CA [km²]	Nights	Time [h]	Meteors
MACMA	Maciejewski	Chełm/PL	Pav35 (0.8/3.8)	5495	4.0	1584	26	196.3	864
			Pav36 (0.8/3.8)*	5668	4.0	1573	26	220.1	1445
			Pav43 (0.75/4.5)*	3132	3.1	319	24	198.0	808
			Pav60 (0.75/4.5)	2250	3.1	281	28	214.2	1328
MARGR	Maravelias	Lofoupoli-Crete/GR	Loomecon (0.8/12)	738	6.3	2698	23	176.8	405
MARRU	Marques	Lisbon/PT	Cab1 (0.8/3.8)	5291	3.1	467	3	22.0	69
			Ran1 (1.4/4.5)	4405	4.0	1241	11	62.8	272
MASMI	Maslov	Novosibirsk/RU	Nowatec (0.8/3.8)	5574	3.6	773	12	44.2	331
MOLSI	Molau	Seysdorf/DE	Avis2 (1.4/50)*	1230	6.9	6152	24	150.6	1144
			Escimo (0.6/130)	21	10.0	3507	2	17.0	10
			Mincam1 (0.8/8)	1477	4.9	1084	24	131.2	571
		Ketzür/DE	Remo1 (0.8/8)	1467	6.5	5491	25	156.9	1326
			Remo2 (0.8/8)	1478	6.4	4778	24	156.3	945
			Remo3 (0.8/8)	1420	5.6	1967	15	96.8	578
			Remo4 (0.8/8)	1478	6.5	5358	24	163.2	1180
MORJO	Morvai	Fülöpszállás/HU	Huful (1.4/5)	2522	3.5	532	20	138.8	261
MOSFA	Moschner	Rovereto/IT	Rover (1.4/4.5)	3896	4.2	1292	17	37.6	327
OCHPA	Ochner	Albiano/IT	Albiano (1.2/4.5)	2944	3.5	358	21	125.8	521
OTTMI	Otte	Pearl City/US	Orie1 (1.4/5.7)	3837	3.8	460	20	133.7	331
PERZS	Perkó	Becsehely/HU	Hubec (0.8/3.8)*	5498	2.9	460	21	151.8	866
PUCRC	Pucer	Nova vas nad Dragonjo/SI	Mobcam1 (0.75/6)	2398	5.3	2976	20	130.3	508
ROTEC	Rothenberg	Berlin/DE	Armefa (0.8/6)	2366	4.5	911	13	78.9	244
SARAN	Saraiva	Carnaxide/PT	Ro1 (0.75/6)	2362	3.7	381	20	173.7	292
			Ro2 (0.75/6)	2381	3.8	459	20	189.4	513
			Ro3 (0.8/12)	710	5.2	619	20	187.9	721
			Sofia (0.8/12)	738	5.3	907	19	145.9	402
SCALE	Scarpa	Alberoni/IT	Leo (1.2/4.5)*	4152	4.5	2052	7	29.6	123
SCHHA	Schremmer	Niederkrüchten/DE	Doraemon (0.8/3.8)	4900	3.0	409	28	134.1	662
SLAST	Slavec	Ljubljana/SI	Kayak1 (1.8/28)	563	6.2	1294	17	92.9	163
STOEN	Stomeo	Scorze/IT	Min38 (0.8/3.8)	5566	4.8	3270	23	137.7	1092
			Noa38 (0.8/3.8)	5609	4.2	1911	28	172.1	1268
			Sco38 (0.8/3.8)	5598	4.8	3306	28	172.5	1651
STORO	Štork	Ondřejov/CZ	Ond1 (1.4/50)*	2195	5.8	4595	1	8.0	81
STRJO	Strunk	Herford/DE	Mincam2 (0.8/6)	2354	5.4	2751	27	143.3	551
			Mincam3 (0.8/6)	2338	5.5	3590	28	138.1	680
			Mincam4 (1.0/2.6)	9791	2.7	552	26	129.7	465
			Mincam5 (0.8/6)	2349	5.0	1896	24	133.6	538
			Mincam6 (0.8/6)	2395	5.1	2178	28	146.6	513
TEPIS	Tepliczky	Agostyán/HU	Huago (0.75/4.5)	2427	4.4	1036	23	134.2	374
			Humob (0.8/6)	2388	4.8	1607	26	154.2	480
TRIMI	Triglav	Velenje/SI	Sraka (0.8/6)*	2222	4.0	546	17	66.1	202
YRJIL	Yrjölä	Kuusankoski/FI	Finexcam (0.8/6)	2337	5.5	3574	14	92.6	387
ZELZO	Zelko	Budapest/HU	Huvcse03 (1.0/4.5)	2224	4.4	933	5	16.1	44
			Huvcse04 (1.0/4.5)	1484	4.4	573	4	15.8	43
* active field of view smaller than video frame						Overall	31	11 199.1	51 979

The International Meteor Organization

web site http://www.imo.net

Council

President: Cis Verbeeck,
Bogaertsheide 5, 2560 Kessel, Belgium.
e-mail: cis.verbeeck@scarlet.be

Vice-President: Jürgen Rendtel,
Eschenweg 16, D-14476 Marquardt, Germany.
tel. +49 33208 50753
e-mail: jrendtel@aip.de

Secretary-General: Robert Lunsford,
1828 Cobblecreek Street, Chula Vista,
CA 91913-3917, USA. tel. +1 619 585 9642
e-mail: lunro.imo.usa@cox.net

Treasurer: Marc Gyssens, Heerbaan 74,
B-2530 Boechout, Belgium.
e-mail: marc.gyssens@uhasselt.be
BIC: GEBABEBB
IBAN: BE30 0014 7327 5911
Always state BIC and IBAN codes together!
Check international transfer charges with your bank; you are responsible for paying these.

Other Council members:
David Asher, Armagh Observatory, College Hill, Armagh, Northern Ireland BT61 9DG, UK.
e-mail: dja@arm.ac.uk
Geert Barentsen, University of Hertfordshire, Hatfield AL10 9AB, UK. e-mail: geert@barentsen.be
Javor Kac (see details under WGN)
Detlef Koschny, Zeestraat 46,
NL-2211 XH Noordwijkerhout, Netherlands.
e-mail: detlef.koschny@esa.int
Sirko Molau, Abenstalstraße 13b, D-84072 Seysdorf, Germany. e-mail: sirko@molau.de
Jean-Louis Rault, Société Astronomique de France, 16, rue de la Vallée, 91360 Epinay sur Orge, France. e-mail: f6agr@orange.fr
Paul Roggemans (see details under IMC Liaison Officer)

Commission Directors

Visual Commission: Rainer Arlt (rarlt@aip.de)
Generic e-mail address: visual@imo.net
Electronic visual report form:
http://www.imo.net/visual/report/electronic
Video Commission: Sirko Molau (sirko@molau.de)
Generic e-mail address: video@imo.net
Photographic Commission: Bill Ward
(William.Ward@glasgow.ac.uk)
Generic e-mail address: photo@imo.net
Radio Commission: Jean-Louis Rault (f6agr@orange.fr)
Generic e-mail address: radio@imo.net
Fireballs: Online fireball reports: coming soon

IMC Liaison Officer

Paul Roggemans, Pijnboomstraat 25, 2800 Mechelen, Belgium, e-mail: paul.roggemans@gmail.com

WGN

Editor-in-chief: Javor Kac
Na Ajdov hrib 24, SI-2310 Slovenska Bistrica, Slovenia. e-mail: wgn@imo.net;
include METEOR in the e-mail subject line

Editorial board: Ž. Andreić, M. Argo, D.J. Asher, J. Correira, M. Gyssens, H.V. Hendrix, C. Hergenrother, T. Markham, J. Rendtel, J.-L. Rault, P. Roggemans, C. Verbeeck.

IMO Sales

Available from the Treasurer or the Electronic Shop on the IMO Website	€	$
IMO membership, including subscription to WGN Vol. 43 (2015)		
Surface mail	26	39
Air Mail (outside Europe only)	49	69
Electronic subscription only	21	29
Back issues of WGN on paper (price per complete volume)		
Vols. 26 (1998) – 35 (2007) except 30 (2002), 38 (2010) – 42 (2014)	15	23
Vols. 37 (2009) – 42 (2014) – electronic version only	9	13
Proceedings of the International Meteor Conference on paper		
1990, 1991, 1993, 1995, 1996, 1999, 2000, 2002, 2003, per year	9	13
2007, 2010, 2011, per year	15	23
2012, 2013, 2014 per year	25	37
Proceedings of the Meteor Orbit Determination Workshop 2006	15	23
Radio Meteor School Proceedings 2005	15	23
Handbook for Meteor Observers	15	23
Meteor Shower Workbook	12	18
Electronic media		
Meteor Beliefs Project CD-ROM	6	9
DVD: WGN Vols. 6–30 & IMC 1991, 1993–96, 2001–04	45	69

Distribution of apparent radiants

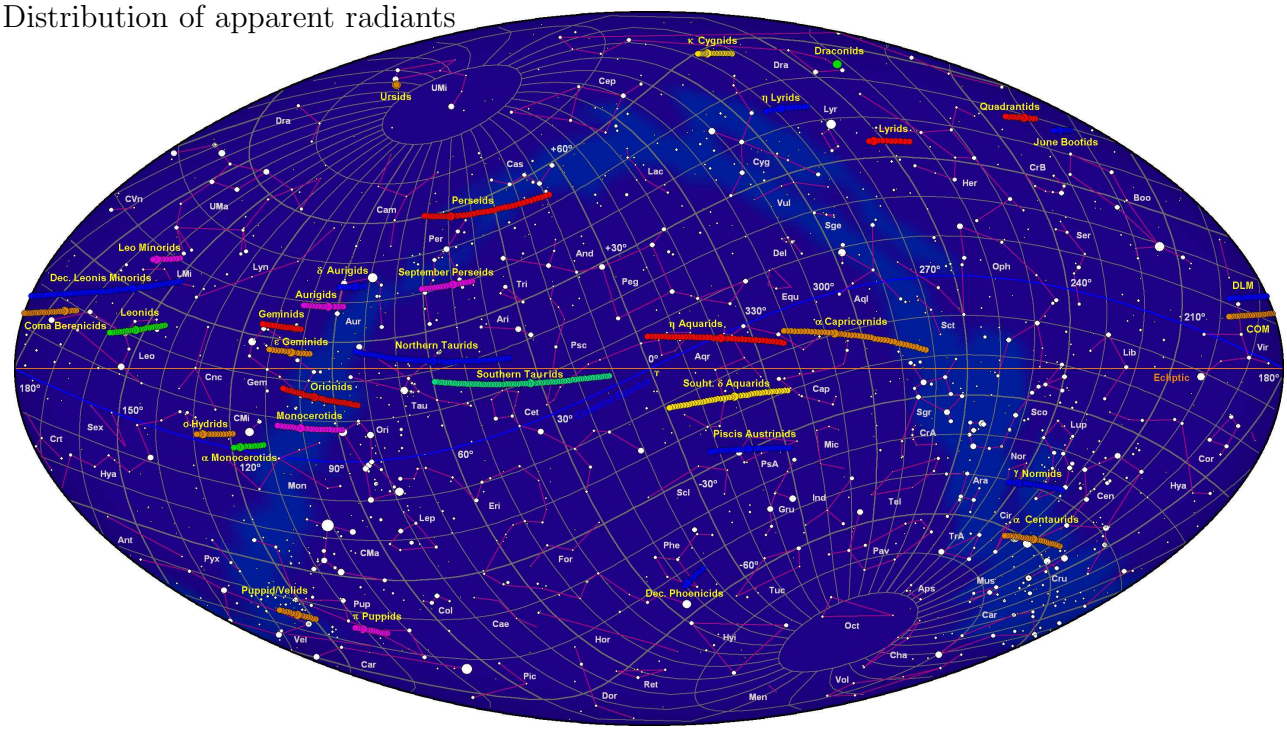

Distribution of geocentric radiants

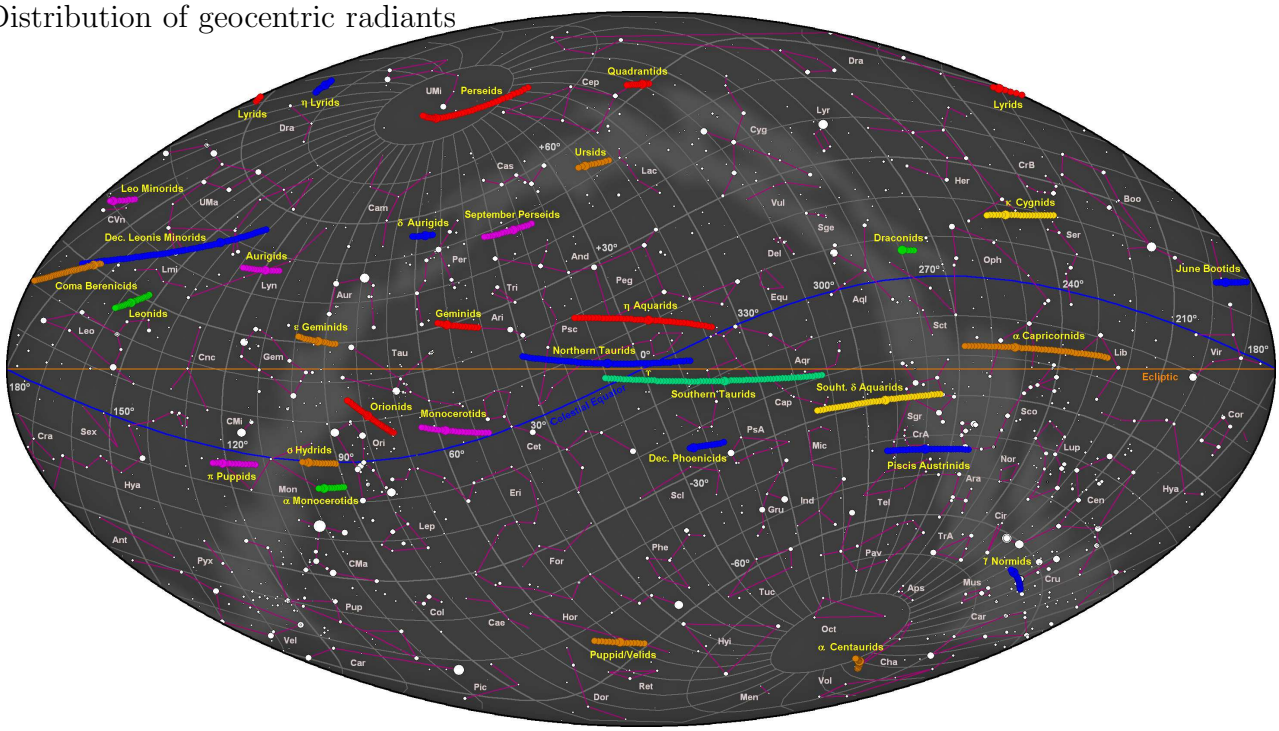

Distribution of sporadic radiants